Introduction to physics of atom/molecule under intense laser pulses

- Above-Threshold-Ionization (ATI) and High-order Harmonic Generation (HHG)
- Attosecond pulse train (APT),single attosecond pulse (SAP)
- Theoretical methods : TDSE, momentum-space, SFA, soft-photon approximation (laser-assisted ionization)
- Conclusions
- Acknowledgements

Photoelectric Effect :

Expt. : Hertz 1887,
Lennard 1900,

Theory : Einstein 1905

$\mathcal{E}_{max} = h\nu - W$

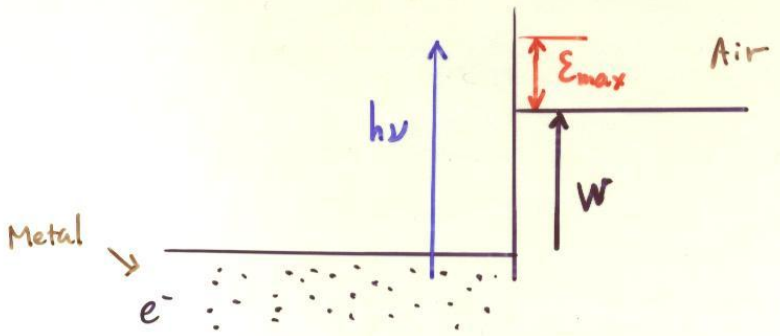

Atomic photoionization 1930 ~ 1960 ±

Typical photoionization cross section:

$X_e + h\nu \longrightarrow X_e^+ + e^-$

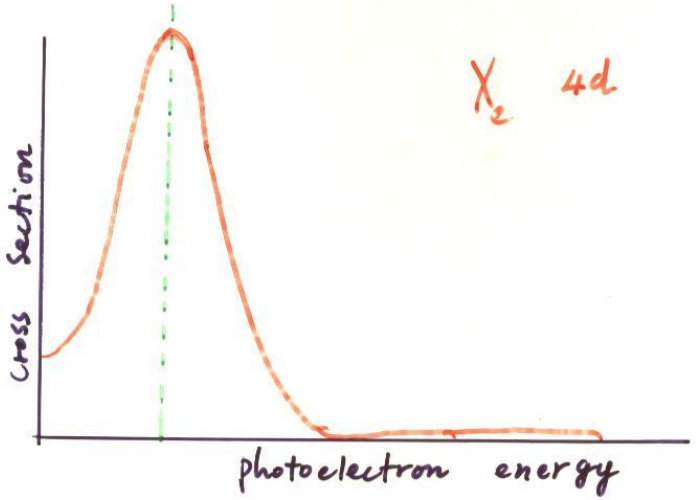

Light Sources by 2000

1. The advent of lasers in 1960 revolutionized the field of spectroscopy. During the past two decades the field has grown explosively.
2. The light field amplitude equals the atomic Coulomb field about 10^9 volts/cm at power level of 10^{15} watts/cm^2 .
3. Current source reaches 10^{18} to 10^{20} watts/cm^2 . It is about one-joule 10-fs focused pulse.

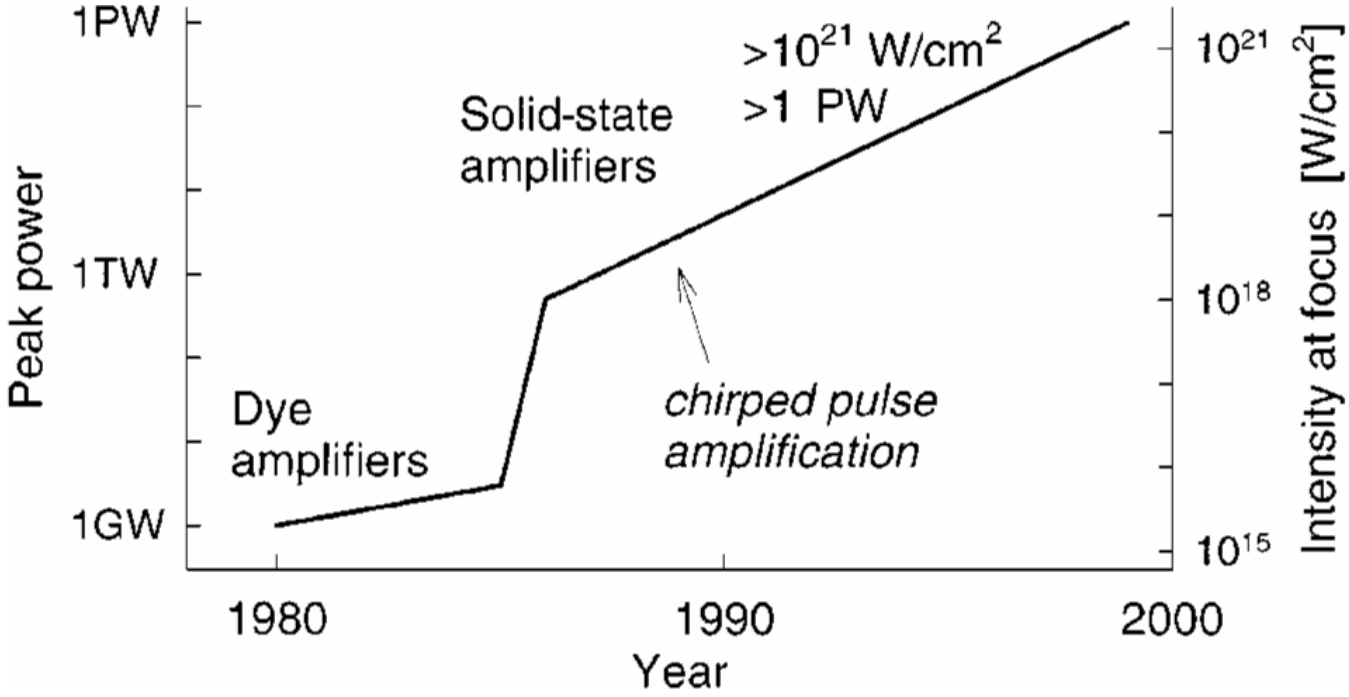

Evolution of ultrashort-pulse amplification in terms of peak power and achievable peak intensity.

Ferenc Krausz and Misha Ivanov: Attosecond physics

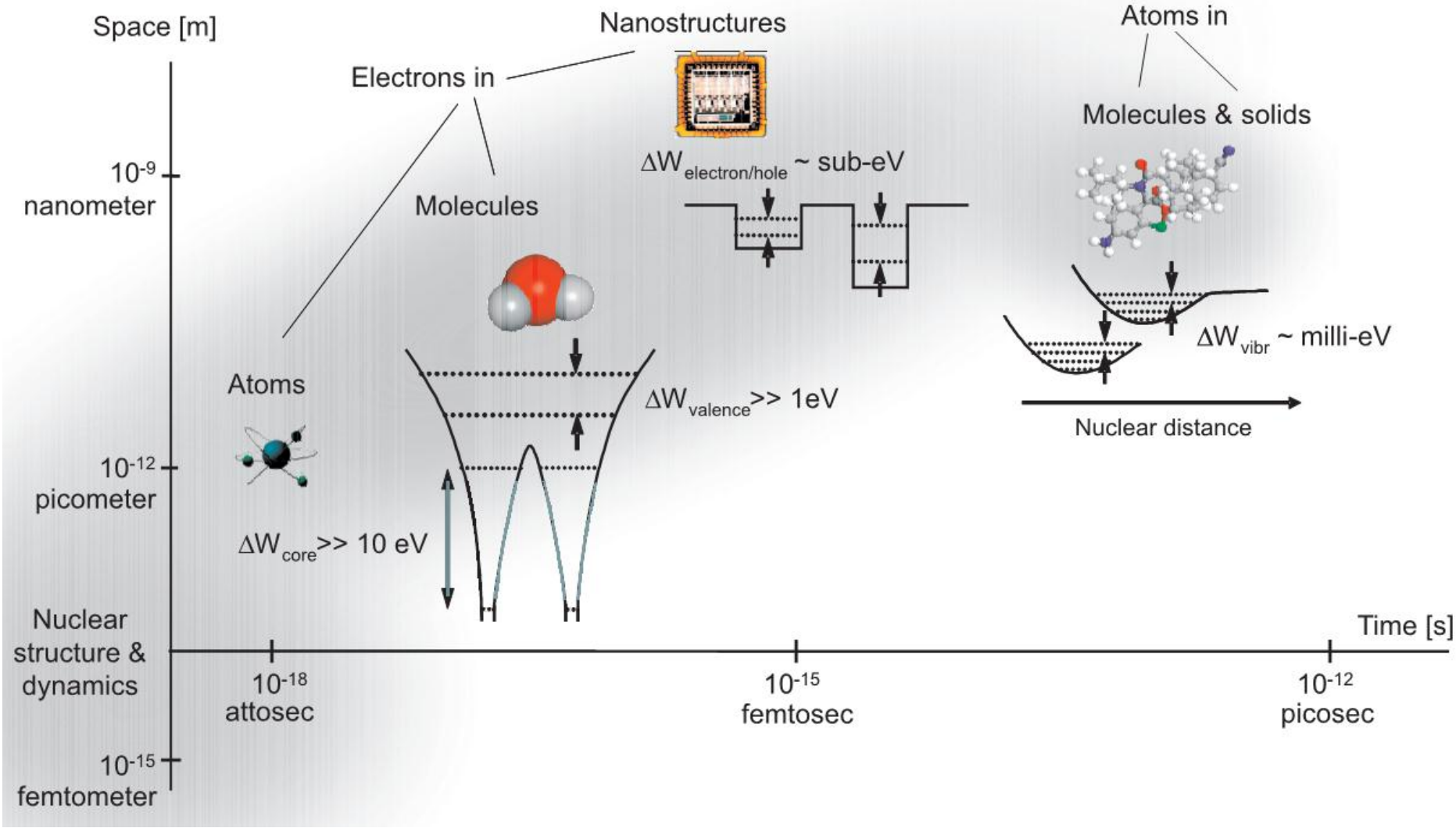

Atomic processes in intense (IR) laser fields

Higher Intensities

Moderate Intensities

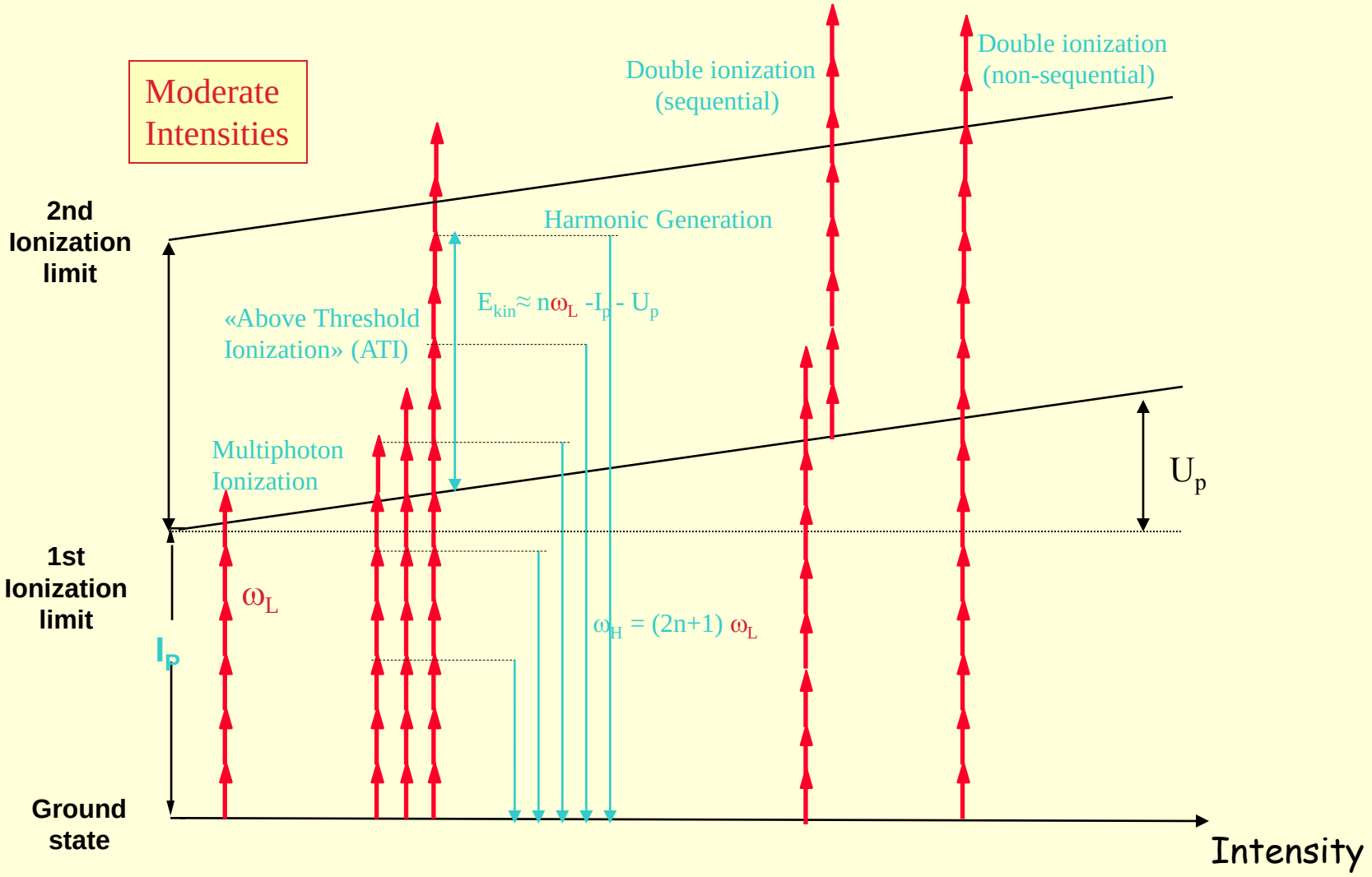

From Maquet's

Due to the laser technology,
the groups at Paris and Moscow
started MPI expt. around 1979.

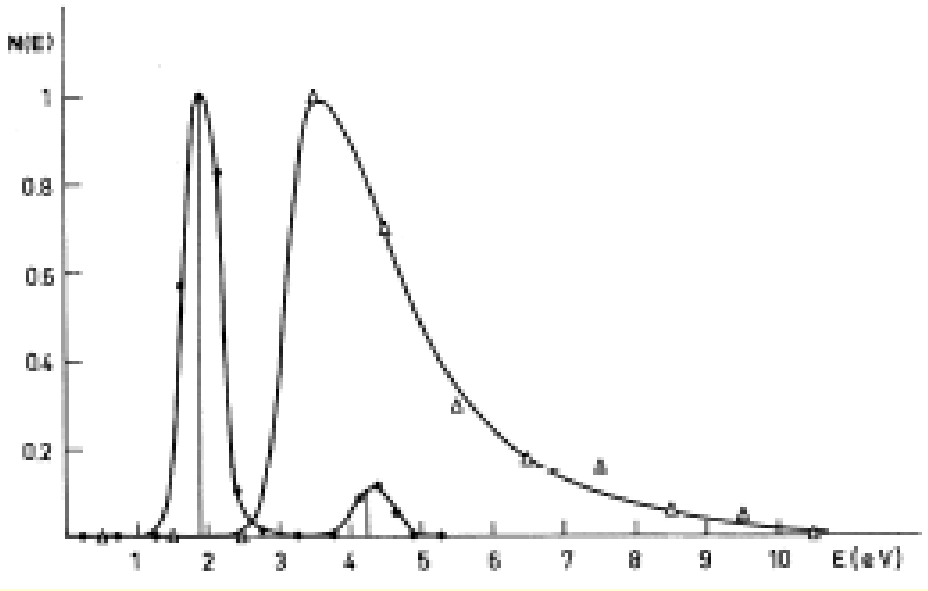

FIG. 3. Energy spectra of the emitted electrons for two photon energies: triangles, $\hbar\omega = 1.17$ eV, $I = 4\times10^{13}$ W/cm^{-2}, $E_{max} = 4$ eV; circles, $\hbar\omega = 2.34$ eV, $I = 8\times10^{12}$ W/cm^{-2}, $E_{max} = 0.2$ eV (E_{max} is the maximum energy

Agostini et al. PRL42, 1127 (1979).

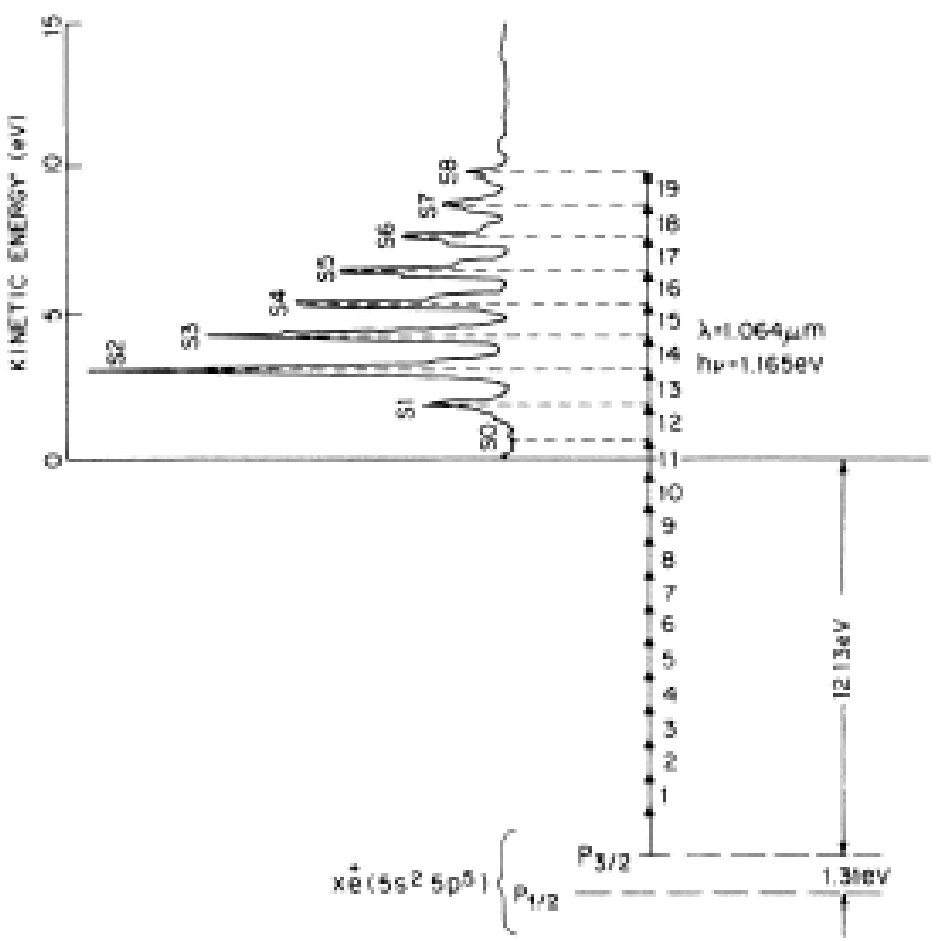

FIG. 1. A schematic of the ATI process for xenon irradiated by intense 1064-nm light. The (doublet) peaks are labeled by $S\mathcal{N}$ where $\mathcal{N}$ is the number of photons absorbed beyond that just necessary to ionize the atom at low intensities. The energy scale is the kinetic energy of the free electron. The two

Freeman et al. PRL 57, 3156 (1986).

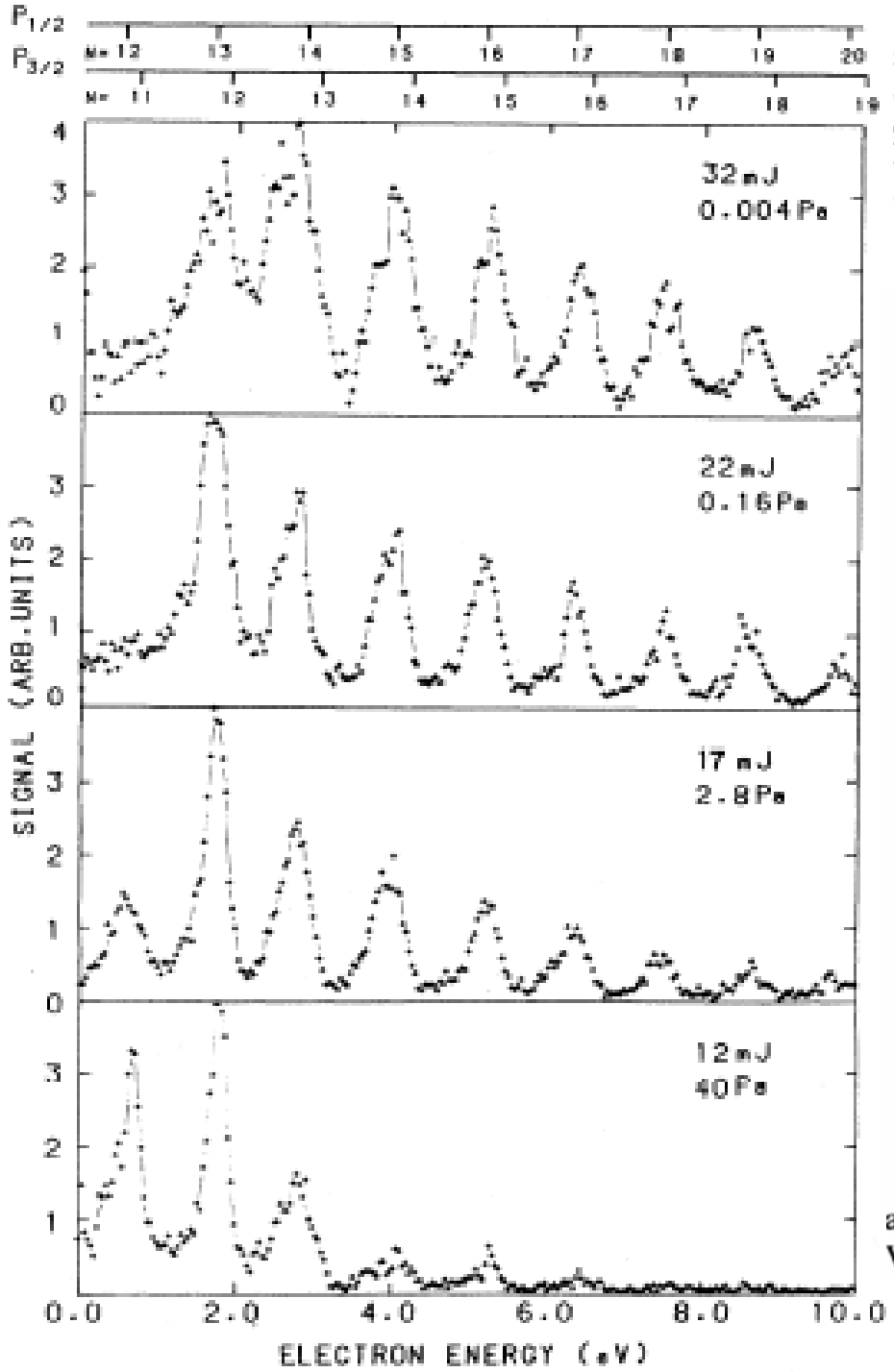

3. Electron spectra from multiphoton ionization of xenon at 1064-nm. The vertical scales are normalized. The pulse energy F and pressure at which each spectrum is taken is given in the figure. In the spectrum at 0.004 Pa, the background has been subtracted. The estimated intensity is $F(\mathrm{mJ}) \times 2.10^{12}$ W/cm^2.

Kruit et al. PRA28, 248 (1983).

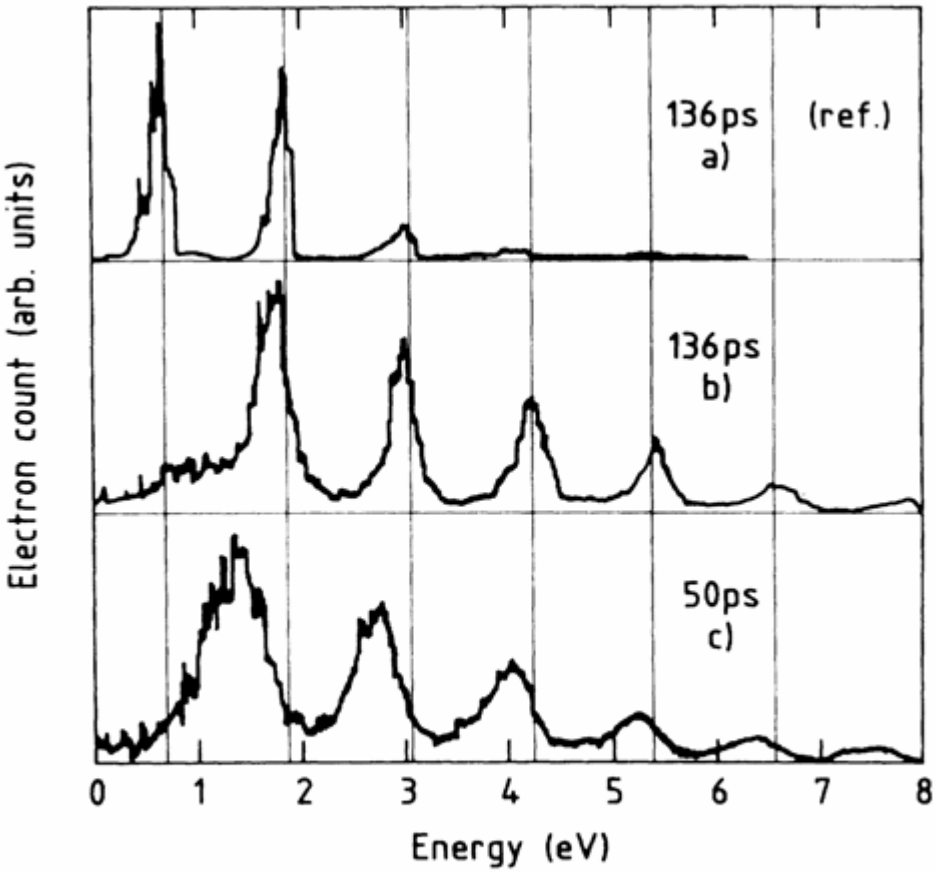

FIG. 2. Electron energy spectra for different laser intensities and pulse durations. (a) reference spectrum, $I = 2.2 \times 10^{12}$ W cm^{-2}; (b) and (c) $I = 7.5 \times 10^{12}$ W cm^{-2}.

PRA36,4111 (1987).

Under laser light, ground state shifts little, Rydberg states and threshold shift up by the ponderomotive energy

ponderomotive potential. In atomic units,

$$U_p = \frac{I}{4\omega^2} = \frac{\langle \mathbf{E}^2 \rangle}{2\omega^2} = \left(\frac{E_0}{2\omega}\right)^2.$$

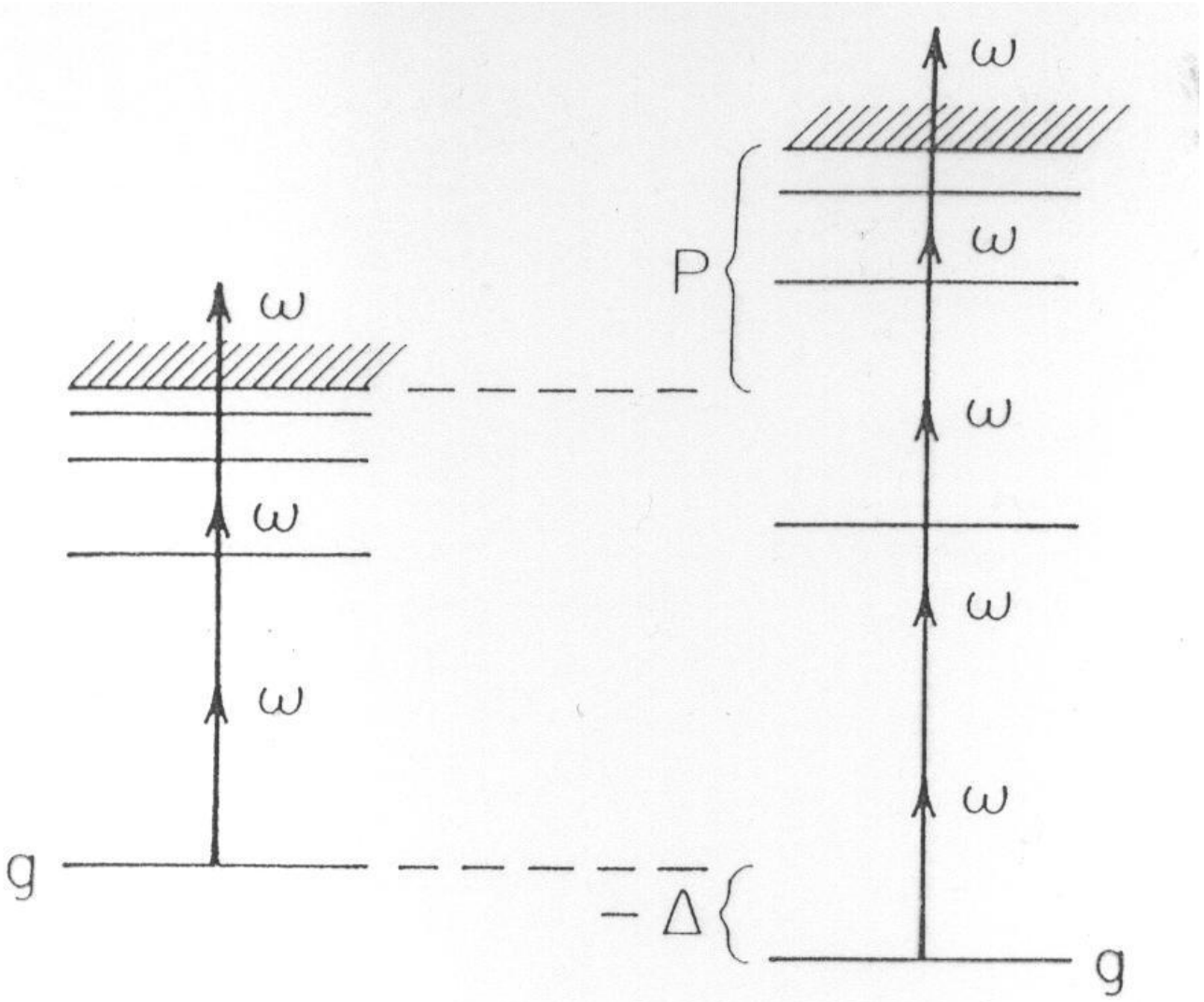

TABLE I. Intensity-dependent complex quasienergy (E_R, $-i\Gamma/2$) in atomic units of the perturbed ground state of the H atom nearby the $N_m=1$ region ($\omega\sim0.5$ a.u.). The rms field strength of $F_{\text{rms}}=1.0$ a.u. corresponds to an rms intensity of 7.0×10^{16} W/cm^2.

ω	E_R	$-\Gamma/2$	ω	E_R	$-\Gamma/2$
	$F_{\text{rms}}=0.01$[a] a.u.			$F_{\text{rms}}=0.05$[a] a.u.	
0.60	−0.499 835 1	−0.1253(−3)[b]	0.60	−0.495 844	−0.3144(−2)
0.55	−0.499 810 4	−0.1729(−3)	0.55	−0.495 201	−0.4355(−2)
0.50	−0.499 784 3	−0.2456(−3)	0.50	−0.494 544	−0.6244(−2)
0.495	−0.499 781 8	−0.2551(−3)	0.495	−0.494 514	−0.6414(−2)
0.490	−0.499 780 4	−0.2647(−3)	0.490	−0.494 380	−0.6510(−2)
	$F_{\text{rms}}=0.025$[a] a.u.			$F_{\text{rms}}=0.075$[c] a.u.	
0.60	−0.498 967	−0.7836(−3)	0.70	−0.492 93	−0.3966(−2)
0.55	−0.498 812	−0.1083(−2)	0.60	−0.490 55	−0.7107(−2)
0.50	−0.498 646	−0.1540(−2)	0.55	−0.489 02	−0.9885(−2)
0.495	−0.498 630	−0.1599(−2)	0.50	−0.487 03	−0.1391(−1)
0.490	−0.498 620	−0.1666(−2)	0.495	−0.486 43	−0.1463(−1)
			0.490	−0.485 57	−0.1588(−1)

[a]For these field strengths, five Floquet blocks (A, $A\pm2\omega$, $A\pm4\omega$) were used with the A's defined by use of 15s, 15p, 15d, 15f, 15g atomic L^2 functions with $\lambda=1.2$ and $\alpha=0.45$ rad.
[b]$-0.1253(-3)\equiv-0.1253\times10^{-3}$.
[c]Six Floquet blocks (A, $A\pm2\omega$, $A\pm4\omega$, $A-6\omega$) were used with each containing 20s, 20p, 20d, 20f, 20g, 20h atomic L^2 functions with $\lambda=1.2$ and $\alpha=0.45$ rad.

Shih-I Chu et al, PRA32, 2769 (1985).

Atomic High-order Harmonic Generations :

① McPherson et al., JOSA B4, 595 (1987) :

Mainfray et al., Scalay group : 1064 nm on Ar, Kr, Xe,

① Use KrF 248 nm, 300 fs, 10^{15} W/cm^2 laser pulse on noble gas (Ne), 17 harmonics (12-photon above threshold) are observed.

general picture :

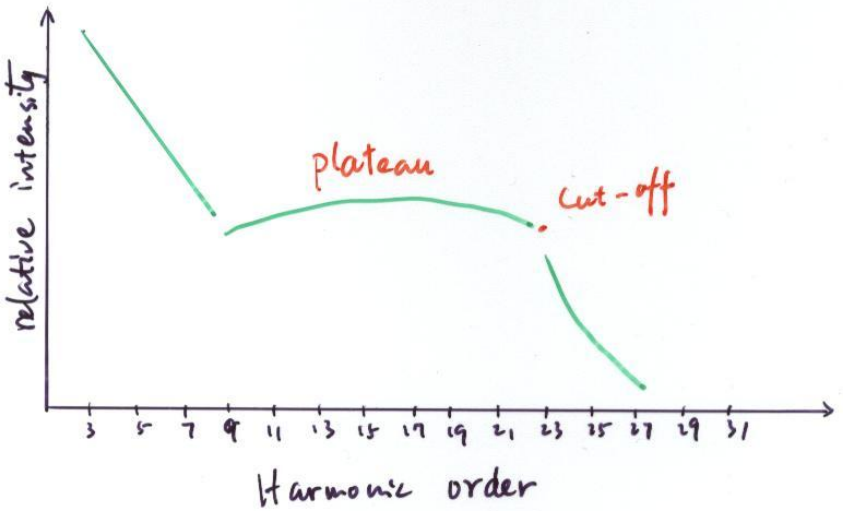

The cut-off order

$$N_{max} = (I_p + 3.17\, U_p) / \hbar\omega$$

I_p = Ionization potential

$U_p = E^2/4\omega^2$ = ponderomotive potential

Kulander, PRL 70, 1599 (1993).

~ empirical rule

* Corkum, PRL 71, 1994 (1993).

Cut-off : Maximum energy of the electron feed back to the parent ion.

High-order Harmonic Generation (HHG) : Simple-man model

Corkum, PRL 71, 1994 (1993).

The fact that the maximum harmonic order $Nh\upsilon = I_p + 3.17U_p$ is explained by :

1. **Tunnel of electron at time t_s with v=0 from the binding potential, two times per laser cycle**
2. **Acceleration of the free electron by laser field**
3. **Rescattering of electron by the parent ion at later time t**

Burnett etc. PRA54, 742 (1996), Kuchiev etc. PRA60, 3111 (1999).

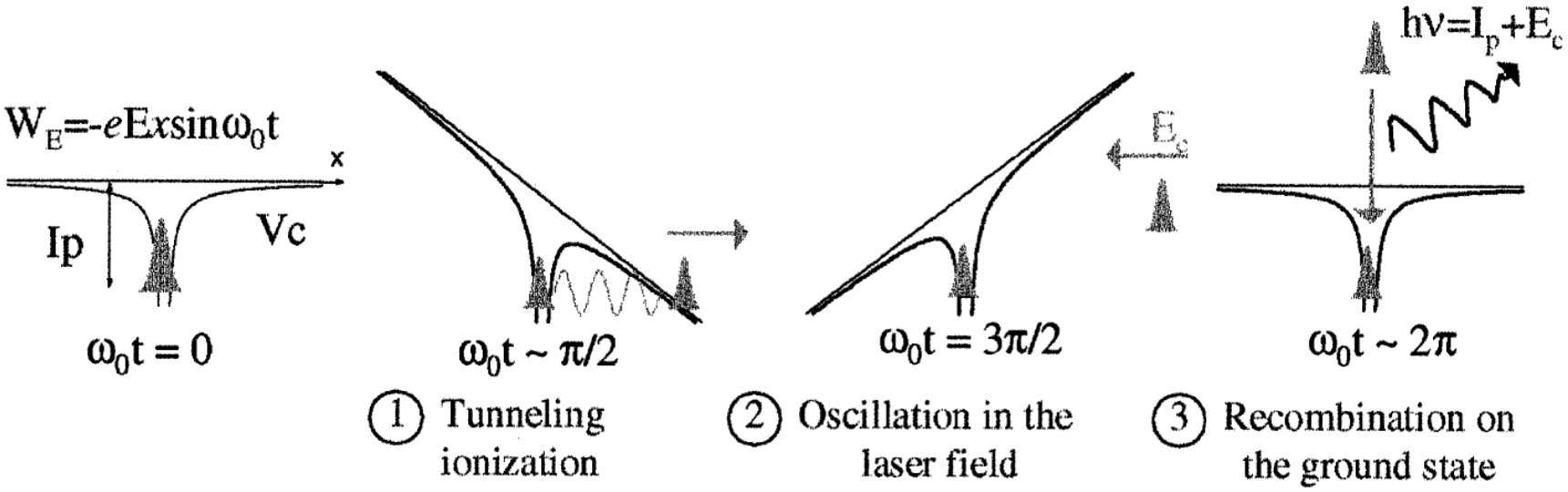

Classical theory I

- 3-step model

$$\ddot{z}(t) = -E_0 \cos \omega t,$$

$$z(t) = z(t_0) + \frac{E_0}{\omega^2}[\cos \omega t - \cos \omega t_0] + \left[\frac{E_0}{\omega}\sin \omega t_0 + \dot{z}(t_0)\right](t - t_0)$$

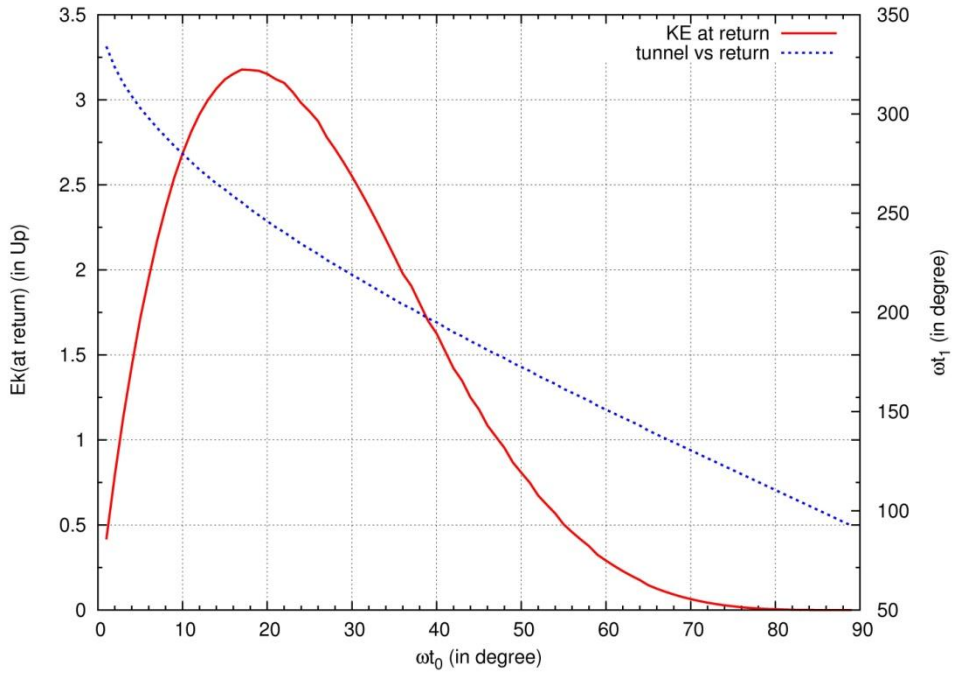

$$\cos \omega t_r - \cos \omega t_0 + \omega \sin \omega t_0 (t_r - t_0) = 0.$$

Maximum Ek(tr) ~ 3.17 Up

Cut-off order of HHG is ~ (3.17Up+Ip)/ω, an empirical fact.

Generation of Coherent X-rays in the Water Window Using 5-Femtosecond Laser Pulses

Ch. Spielmann, N. H. Burnett, S. Sartania, R. Koppitsch,
M. Schnürer, C. Kan, M. Lenzner, P. Wobrauschek, F. Krausz*

Coherent extreme-ultraviolet radiation extending to wavelengths below the carbon K edge at 4.37 nanometers (nm) has been generated at a repetition rate of 1 kilohertz by focusing 5-femtosecond near-infrared (780 nm) laser pulses into a helium gas jet. The incident light field performs just a few oscillations, which results in the emission of an x-ray supercontinuum rather than discrete harmonics. Owing to the extremely short rise time of the driving pulses, neutral atoms can be exposed to high fields before they are depleted by ionization. As a result, the observed x-ray radiation extends well into the water window and is delivered in a well-collimated beam (divergence less than 1 milliradian). The high repetition rate and spatial coherence result in a brightness of about 5×10^8 photons per square millimeter per square milliradian per second in a 1-percent bandwidth at 4.37 nm, the carbon edge of the water window. The compact laboratory system holds promise as a source for biological holography and nonlinear optics in the x-ray regime.

Science278, 661 (1997)

X-ray Pulses Approaching the Attosecond Frontier

Markus Drescher,[1,2] Michael Hentschel,[1] Reinhard Kienberger,[1] Gabriel Tempea,[1] Christian Spielmann,[1] Georg A. Reider,[1] Paul B. Corkum,[3] Ferenc Krausz[1]*

Single soft-x-ray pulses of ~90–electron volt (eV) photon energy are produced by high-order harmonic generation with 7-femtosecond (fs), 770-nanometer (1.6 eV) laser pulses and are characterized by photoionizing krypton in the presence of the driver laser pulse. By detecting photoelectrons ejected perpendicularly to the laser polarization, broadening of the photoelectron spectrum due to absorption and emission of laser photons is suppressed, permitting the observation of a laser-induced downshift of the energy spectrum with sub-laser-cycle resolution in a cross correlation measurement. We measure isolated x-ray pulses of 1.8 (+0.7/−1.2) fs in duration, which are shorter than the oscillation cycle of the driving laser light (2.6 fs). Our techniques for generation and measurement offer sub-femtosecond resolution over a wide range of x-ray wavelengths, paving the way to experimental attosecond science. Tracing atomic processes evolving faster than the exciting light field is within reach.

Science291, 1923 (2001)

How to generate attosecond Pulses?

- **Laser pulse: 5-7 fs, 0.75μm**

$$E(t) = \int d\omega A(\omega) \exp[-i\omega t + i\phi(\omega)]$$

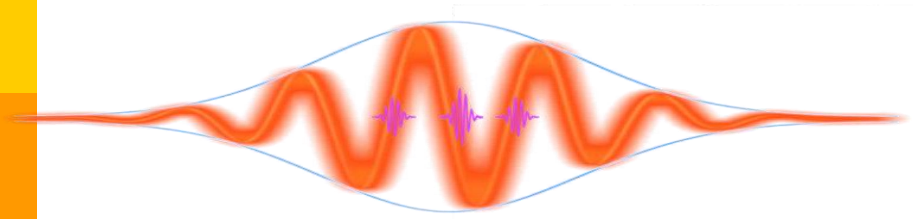

Single attosecond pulse

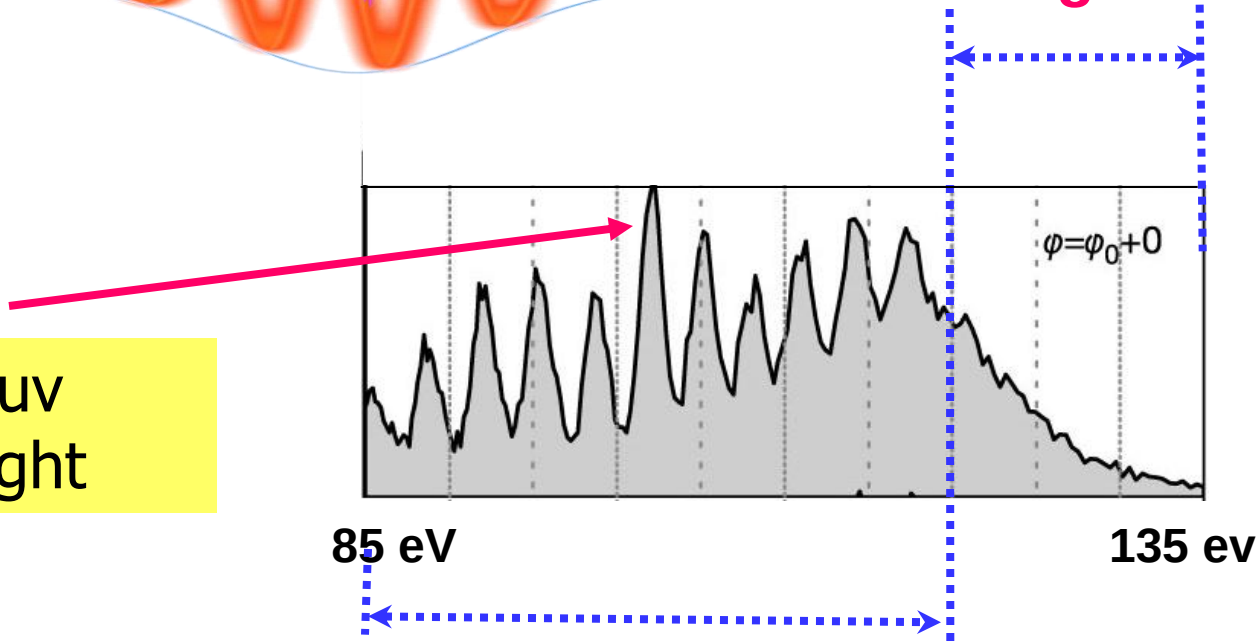

$$E(t) = \sum_N A_q \exp[-iw_q t + i\phi(\omega_q)]$$

From CD Lin

A. BALTU KA *et al.*, Nature **421,** 611(2003)

1. **Need broad-band spectrum**

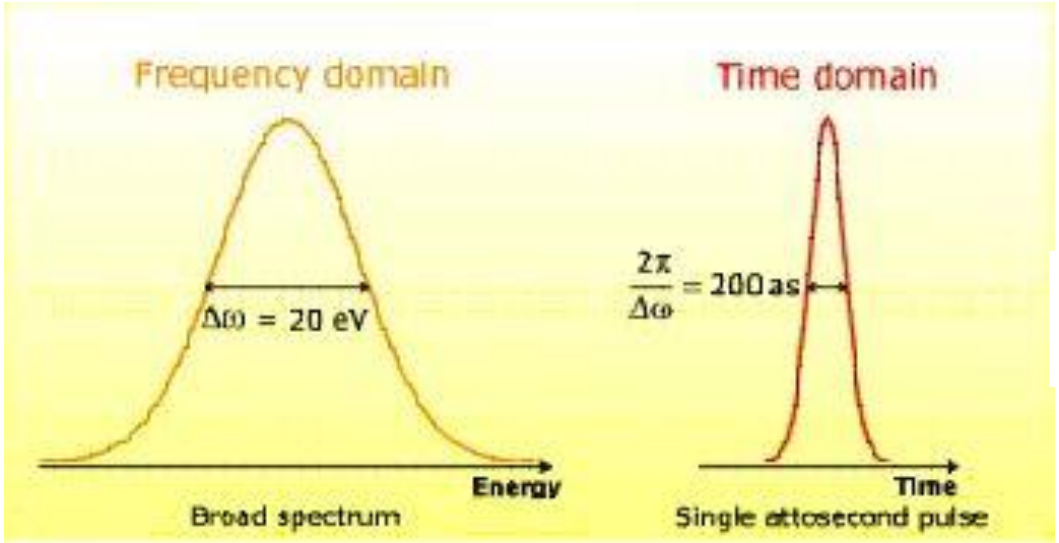

Single as. pulse (SAP)

2. **Phases have to be locked**

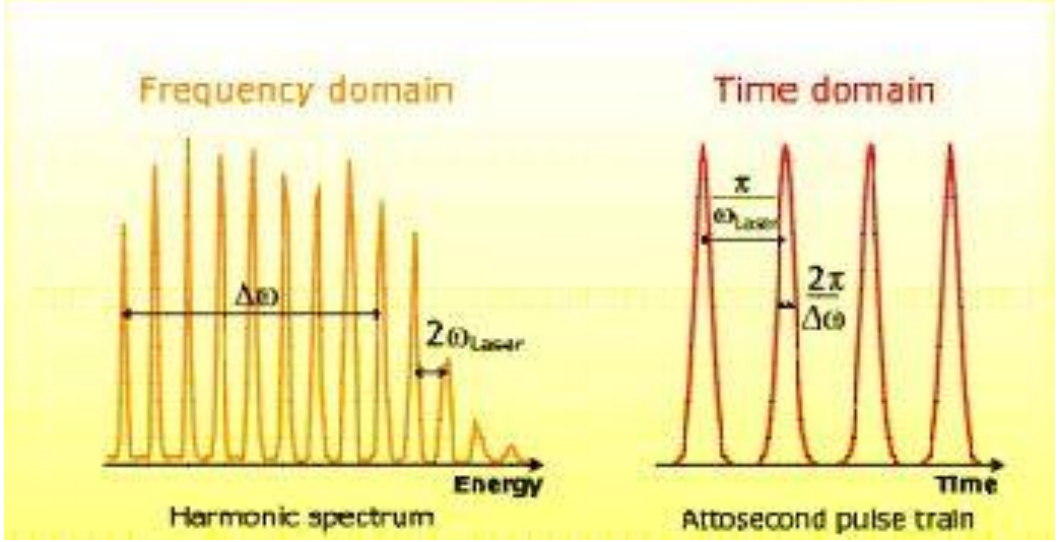

As. Pulse train (APT)

From CD Lin

Synthesis of harmonics into pulse train

$$E(t) = \sum_{n=11}^{29} \sin(n\omega t + \varphi_n), n = odd$$

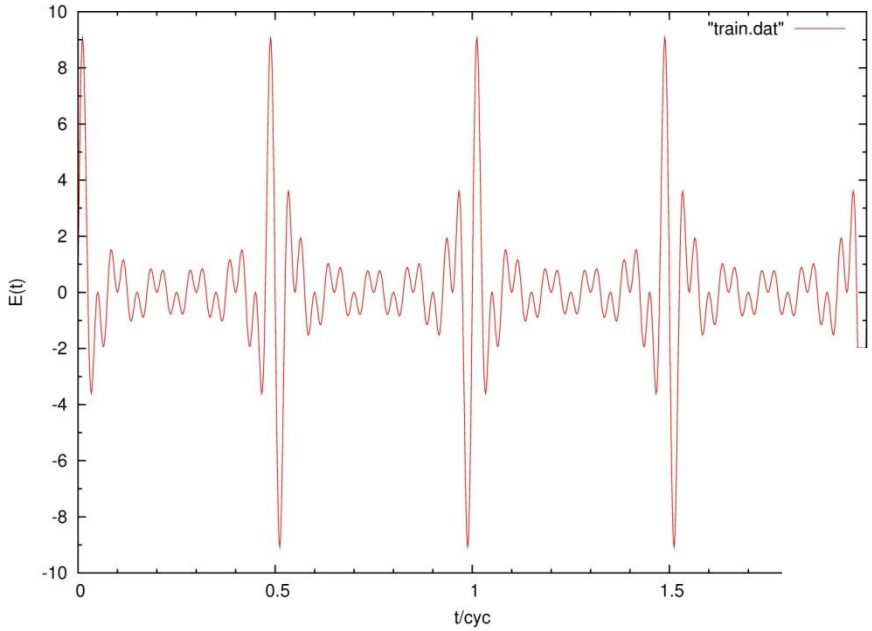

$\varphi_n = \text{constant}$

$\varphi_n = \text{random}$

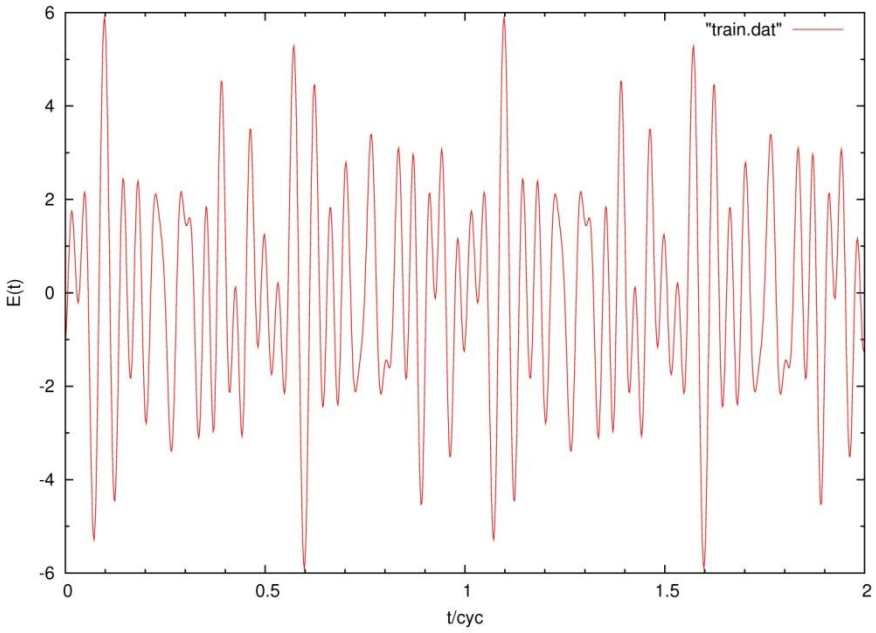

W. Lin and A. Kung, Opt Ex 17, 16342 (2009)

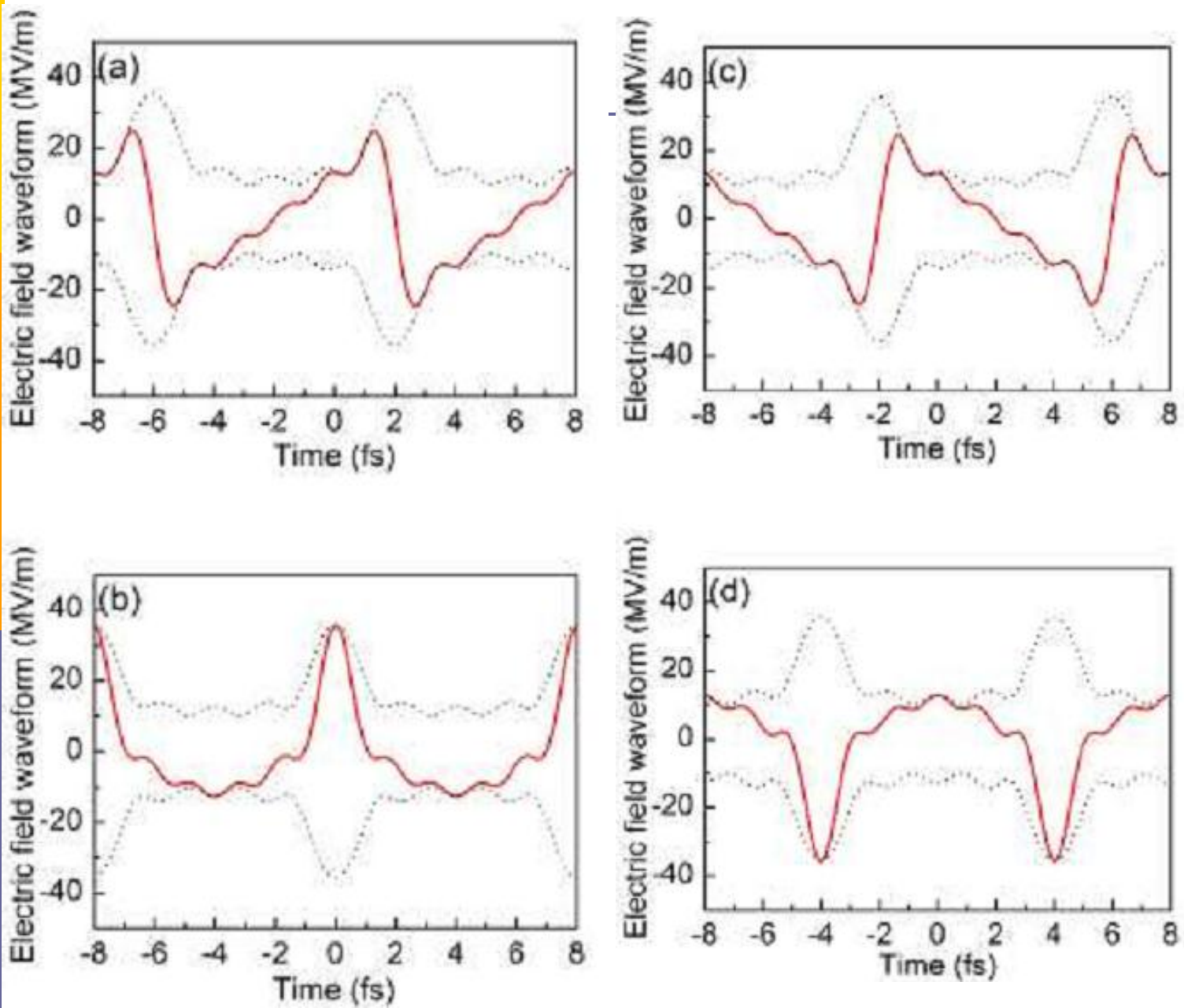

Isolated **attosecond pulses (SAP)**

MPQ (Krausz's group) **90 eV** bandwidth 10 eV

650 as (2001)

250 as (2004)

80 as (2007)

Milano group **36** eV (**Polarization gating**)

130 as (2006) about 1.2 period

KSU (Polarization gating)

two-color + polarization gating (2009}

25 as

From CD Lin

Streak camera, FROG-CRAB

Atom under XUV+weak IR, ionized electron at *ti* is dressed by IR, the velocity at t later is given below. (e < 0) (conjugate momentum p is time constant).

$$\mathbf{v}(t) = -\frac{e}{m_e}\mathbf{A}(t) + \left[\mathbf{v}_0 + \frac{e}{m_e}\mathbf{A}(t_i)\right]$$

Photoelectron spectrum at the end contains information of pulse.
The duration of ultrashort pulse can be measured. *Corkum et al, 2002.*

Using temporal gating technique, a "Frequency-Resolved-Optical-Gating" for "Complete-Reconstruction of Attoesecond-Bursts" FROG-CRAB was developed to trace the attosecond pulse. *Mairsese et al, 2005*

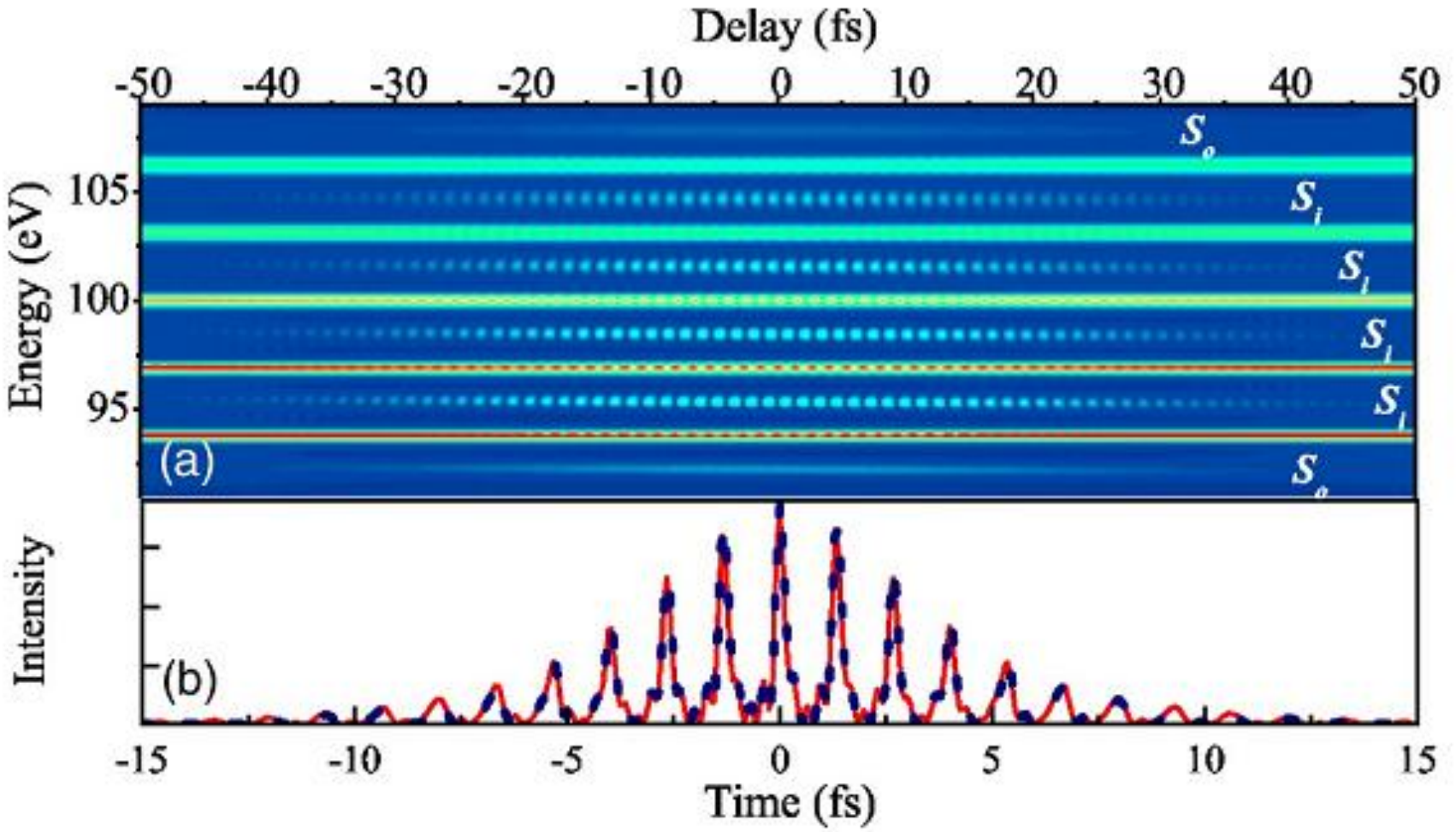

FIG. 2. (a) CRAB trace at $\theta=0$ of a 12-fs-train of nonidentical as pulses, of period $T/2=1.3$ fs, gated by a 30-fs-800 nm- ($T=2.6$ fs) laser pulse, of 0.05 TW/cm^2 peak intensity, assuming a spectrometer resolution of 100 meV. The as pulses are shorter in the center of the train (≈250 as), than in the edges (≈400 as). The

Example of controlled ATI – atomic pump probe

$$E(t) = E_1(t)\sin\omega t + E_h(t - t_d)\sum_q \sin(q\omega[t - t_d] + \phi_q)$$

$E_1(t)$ is IR envelope, *FWHM* ~ *27fs*, intensity ~ 10^{14} *w/cm*^{2} Keller, PRL2004

q=*11-19*, φ_q is fixed relative phase.

E_h is ATP pulse envelope, *FWHM* ~ *14fs*, intensity ~ 10^{13} *w/cm*^{2}

The ionization enhanced by 20-25 for all value of time delay t_d (or τ below)

By tuning time delay, the born electron can be driven by peak or small IR field.

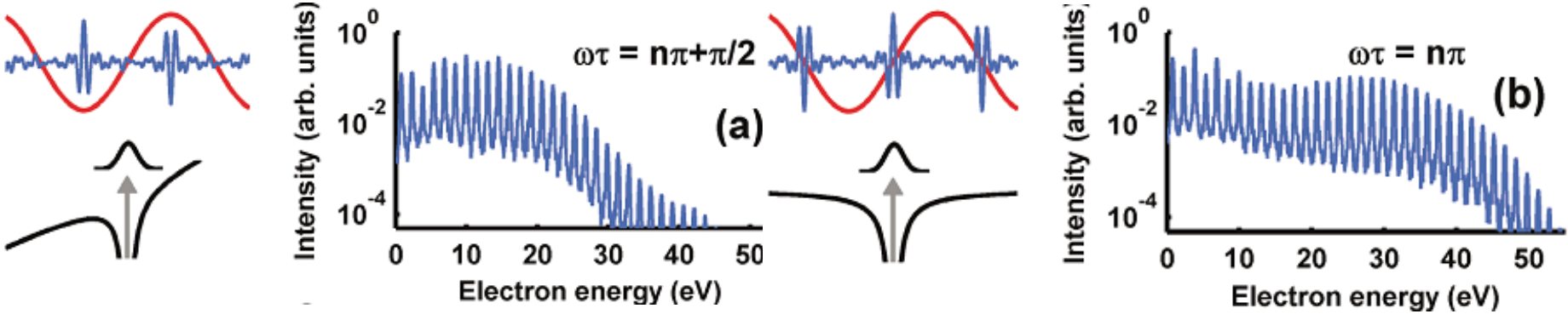

Schafer : TDSE

Attosecond Pulse Train (APT) on helium, argon atoms

$$E(t) = E_1(t)\sin\omega t + E_h(t - t_d)\sum_q \sin(q\omega[t - t_d] + \phi_q)$$

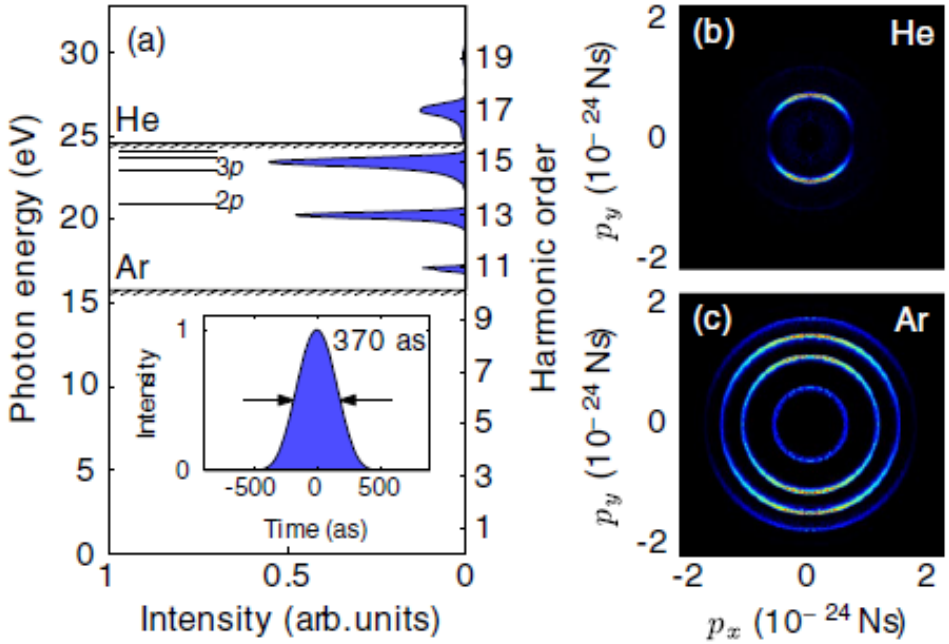

FIG. 1 (color online). (a) Spectrum of the UV pulses used in the experiment shown in relation to the ionization potentials of helium and argon. The inset shows the temporal profile of the attosecond pulses in the train. Experimental photoelectron momentum distributions from single-photon ionization by the APT in helium (b) and argon (c) with the polarization of the light parallel to the p_y axis.

PRL92,023003 (2004)
APT pump + probe pulses

PRL99,233001(2007)
SAP pump + probe

Theoretical Methods : for simple targets

Solving the time-dependent Schrödinger Equation (TDSE)

$$H = H_{atom} + H_i(t)$$

$$H\Psi(\vec{r},t) = i\hbar\frac{\partial}{\partial t}\Psi(\vec{r},t)$$

Limited to one-electron model atomic systems

Time-dependent Density Functional Theory (Chu)

To compare with experiment:

Integrated over laser interaction volume

Validity of the perturbation theory

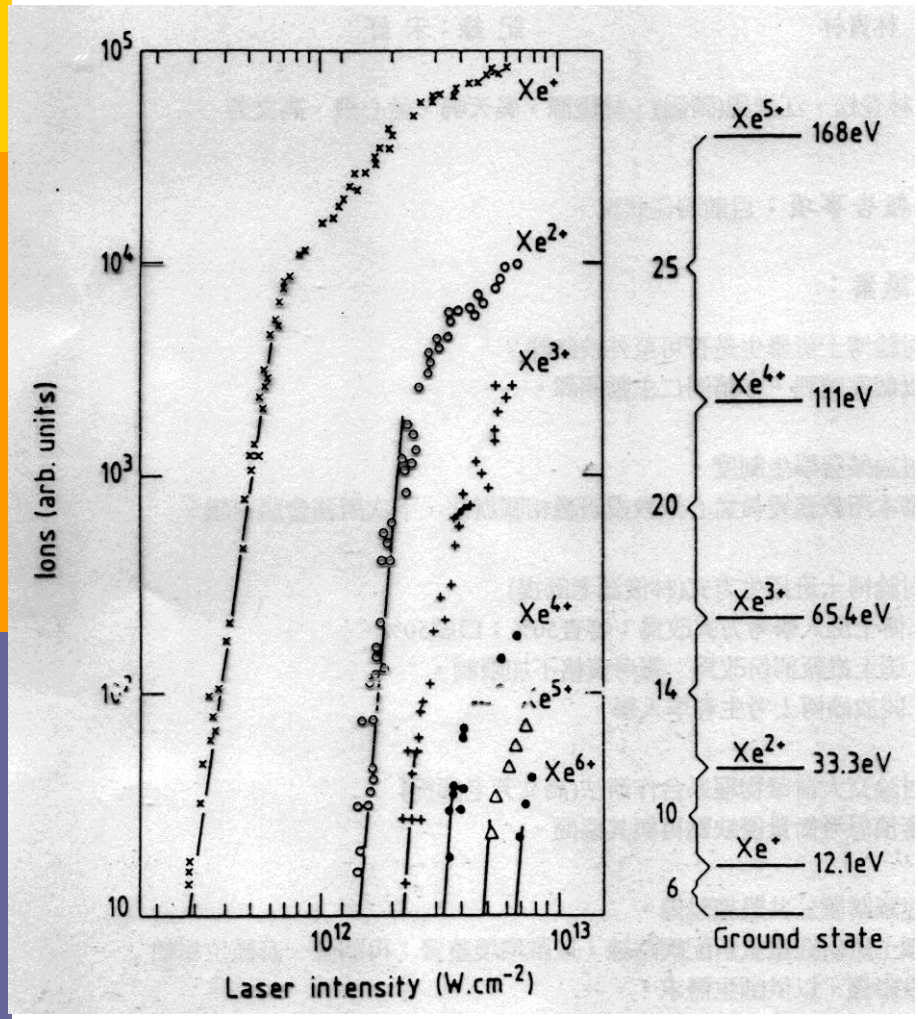

$$R_N = \frac{2\pi}{\hbar}\left(\frac{2e^2}{\varepsilon_0 c}\right)^N I^N \sum_f |M_{i\to f}^{(N)}|^2 = \sigma_N \Phi^N \quad (I = \hbar\omega\Phi)$$

$$M_{i\to f}^{(N)} =$$

$$\sum_{j',j'',\ldots,j'''} \frac{\langle i|x|j'\rangle\langle j'|x|j''\rangle\cdots\langle j'''|x|f\rangle}{(E_i+\hbar\omega-E_{j'})(E_i+2\hbar\omega-E_{j''})\cdots(E_i+(N-1)\hbar\omega-E_{j'''})}$$

The trouble in calculations :

設此 $\lambda = 532$ nm, pulse duration 1 ps,
實驗觀察第 4 個 ATI peak

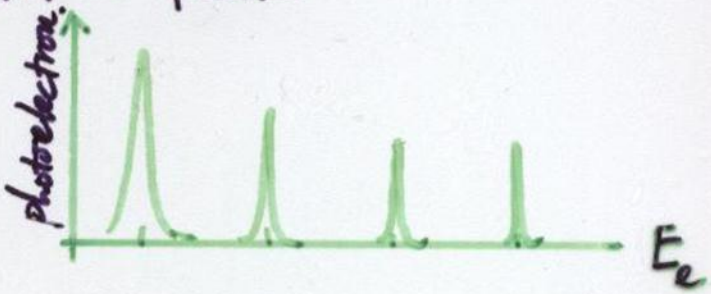

Max. kinetic energy of photo electron

$\sim 4\hbar\omega$

$$p_e = \sqrt{2m E_e} = \sqrt{2 \times 4 \times 0.056} \sim 0.83 \text{ (a.u.)}$$

In 1 ps, (41322 a.u.), the electron wave packet will travel $\sim 0.83 \times 41322 = 34256$ (a.u.)

If take space grid $\Delta x = 0.2$ a.u.

needs $\left[\frac{34256 \times 2}{0.2}\right]^3 \sim 10^{16}$ grid points !

Momentum space method for AMO problems

$$-\frac{1}{2}\nabla^2\Psi(\vec{r}) + V(r)\Psi(\vec{r}) = E\Psi(\vec{r}).$$

Fock, 192?

By making the Fourier transformations,

$$\Phi(\vec{p}) = 1/(2\pi)^{\frac{3}{2}} \int \Psi(\vec{r}) e^{-i\vec{p}\cdot\vec{r}} d^3r\,,$$
$$W(\vec{p}) = 1/(8\pi^3) \int V(\vec{r}) e^{-i\vec{p}\cdot\vec{r}} d^3r\,,$$

$$[\frac{p^2}{2} - E]\Phi(\vec{p}) + \int W(\vec{p}-\vec{q})\Phi(\vec{q}) d^3q = 0\,.$$

for Coulomb potential $V(\vec{r}) = -Z/r$, we

$$\Phi(\vec{p}) = F_{n,l}(p) Y_{lm}(\Omega_p)\,.$$

$$[\frac{p^2}{2} - E]F_{n,l}(p) + \int q^2 K_l(p,q) F_{n,l}(q) dq = 0.$$

$$K_l(p,q) = -\frac{Z}{\pi pq} Q_l(\frac{p^2+q^2}{2pq}), \qquad Q_l(z) = \frac{1}{2}\int_{-1}^{1} \frac{1}{z-x} P_l(x) dx,$$

See also, Pauling etc. PR34,109 (29)

the singularity in $Q_l(z)$ when $z = \frac{p^2+q^2}{2pq} = 1$.

Lande's subtraction method :

$$\int q^2 K_l(p,q) F_{n,l}(q) dq = \int K_l(p,q)[q^2 F_{n,l}(q) - p^2 F_{n,l}(p)/P_l(z)]dq + p^2 F_{n,l}(p) \int \frac{K_l(p,q)}{P_l(z)} dq$$

1. A basis expansion to solve the bound states in momentum space.
2. A few thousands Gauss-Legendre girds were used to find some low-lying energy levels accurately.
3. In intense field problems, basis expansion is incomplete, unless your Hilbert space is represented well. Thousands grid points in each angular momentum state are time consuming.

1. A key correction to the Coulomb kernel in practical computation by finite spatial range was derived.

Finite sphere of radius R : **For infinite R :**

$$W(\vec{p}) = \begin{cases} \frac{\cos(pR)-1}{2\pi^2 p^2} & \text{if } p \neq 0 \\ \frac{-R^2}{4\pi^2} & \text{otherwise} \end{cases} \qquad W(\vec{p}) = \frac{-1}{2\pi^2 p^2}.$$

$$W(\vec{p}-\vec{q}) = \sum_{l=0} a_l(p,q)\, P_l(cos\gamma) \qquad \text{where } \gamma \text{ is the angle between } \vec{p} \text{ and } \vec{q}$$

$$a_l(p,q) = \frac{2l+1}{2} \int_{-1}^{1} W(\vec{p}-\vec{q})\, P_l(x) dx.$$

$$[\frac{p^2}{2} - E] F_{nl}(p) + \frac{4\pi}{2l+1} \int_0^{p_{max}} a_l(p,q) F_{nl}(q) q^2 dq = 0.$$

Discretization, quadrature :

$$[\frac{p_i^2}{2} - E] F_{nl}(p_i) + \frac{4\pi}{2l+1} \sum_{j=1}^{N} w_j\, a_l\,(p_i, p_j)\, q_j^2\, F_{nl}(p_j) = 0,\ i = 1, 2, 3, \cdots, N.$$

2. Use pseudospectral collocation points and bilinear map. Adjust the grids and optimize the favored region.

For x in [-1,1] and p in [0, p_{max}],

With the two modifications, only hundred grid points give highly accurate eigenstates (shown below).

Criterion for the validity of finite R modification :

- p- space Schrödinger eq is subject to the condition

$$1/(8\pi^3)\int_{-L_x}^{L_x} dx \int_{-L_y}^{L_y} dy \int_{-L_z}^{L_z} dz\, e^{i\vec{p}\cdot\vec{r}} = \frac{\sin(p_x L_x)}{\pi p_x}\frac{\sin(p_y L_y)}{\pi p_y}\frac{\sin(p_z L_z)}{\pi p_z} \cong \delta(p_x)\delta(p_y)\delta(p_z).$$

The condition holds only if the box size $L_x L_y L_z$ is large enough.

Oscillator Strength

$$f_{nl\to n',l+1} = \frac{2(l+1)}{3(2l+1)}\frac{1}{E_{n'}-En}\left|\int p\,F_{nl}(p)F_{n',l+1}(p)\right|^2,$$

$$f_{nl\to n',l-1} = \frac{2l}{3(2l+1)}\frac{1}{E_{n'}-En}\left|\int p\,F_{nl}(p)F_{n',l-1}(p)\right|^2.$$

TABLE II: The oscillator strength for the transition from ns-state to np-state. B-S denotes the results in Ref.[6]. $7.91[-2] = 7.91 \times 10^{-2}$.

final	$1s$	B-S	$2s$	B-S	$3s$	B-S	$4s$	B-S
$2p$	0.4162	0.4162	_	_	-4.08[-2]	-4.1[-2]	-9.13[-3]	-0.009
$3p$	7.91[-2]	7.91[-2]	0.4348	0.4349	_	_	-9.68[-2]	-0.097
$4p$	2.90[-6]	2.90[-2]	0.1028	0.1028	0.4846	0.484	_	_
$5p$	1.39[-2]	1.39[-2]	4.19[-2]	4.19[-2]	0.1210	0.121	0.544	0.545
$6p$	7.84[-3]	7.8[-3]	2.17[-2]	2.16[-2]	5.17[-2]	5.2[-2]	0.1388	0.138
$7p$	6.00[-3]	4.8[-3]	1.58[-2]	1.27[-2]	3.38[-2]	2.7[-2]	7.26[-2]	6.0[-2]
discrete sum	0.5668	0.5650	0.6532	0.6489	0.7167	0.707	0.7610	0.752
continuous sum	0.4332	0.4350	0.3468	0.3511	0.2833	0.293	0.239	0.248
total	1.000	1.000	1.000	1.000	1.000	1.000	1.000	1.000

Calculation of ATI photoelectron spectrum

For a hydrogen atom under laser pulse, the time-dep. Schrödinger eq., we use the generated eigenstates as basis for the problem.

Solve the coupled system eqs. of coefficients, the dynamics is feasible to work out on a desktop pc.

Table 5
The four ATI spectra cases

Case	λ (nm)	I_{peak} (w/cm^2)	T (fs)	$l_{\max}$	$P_{l\,\max}$	P_{ionized}
I	400	10^{14}	26.6	11	1.5×10^{-11}	2.15%
II	400	2×10^{14}	26.6	14	3.7×10^{-11}	7.23%
III	400	10^{15}	26.6	39	2.5×10^{-10}	91.97%
IV	608	10^{14}	405	29	4.6×10^{-10}	2.63%

λ is the laser wavelength. I_{peak} is the peak intensity of the laser field. T is the pulse duration in femtoseconds. The angular momenta used in each case are $l = 0, 1, \ldots, l_{\max}$. $P_{l\,\max}$ is the probability of the final state in angular momentum stats of $l = l_{\max}$. P_{ionized} is the ionization probability.

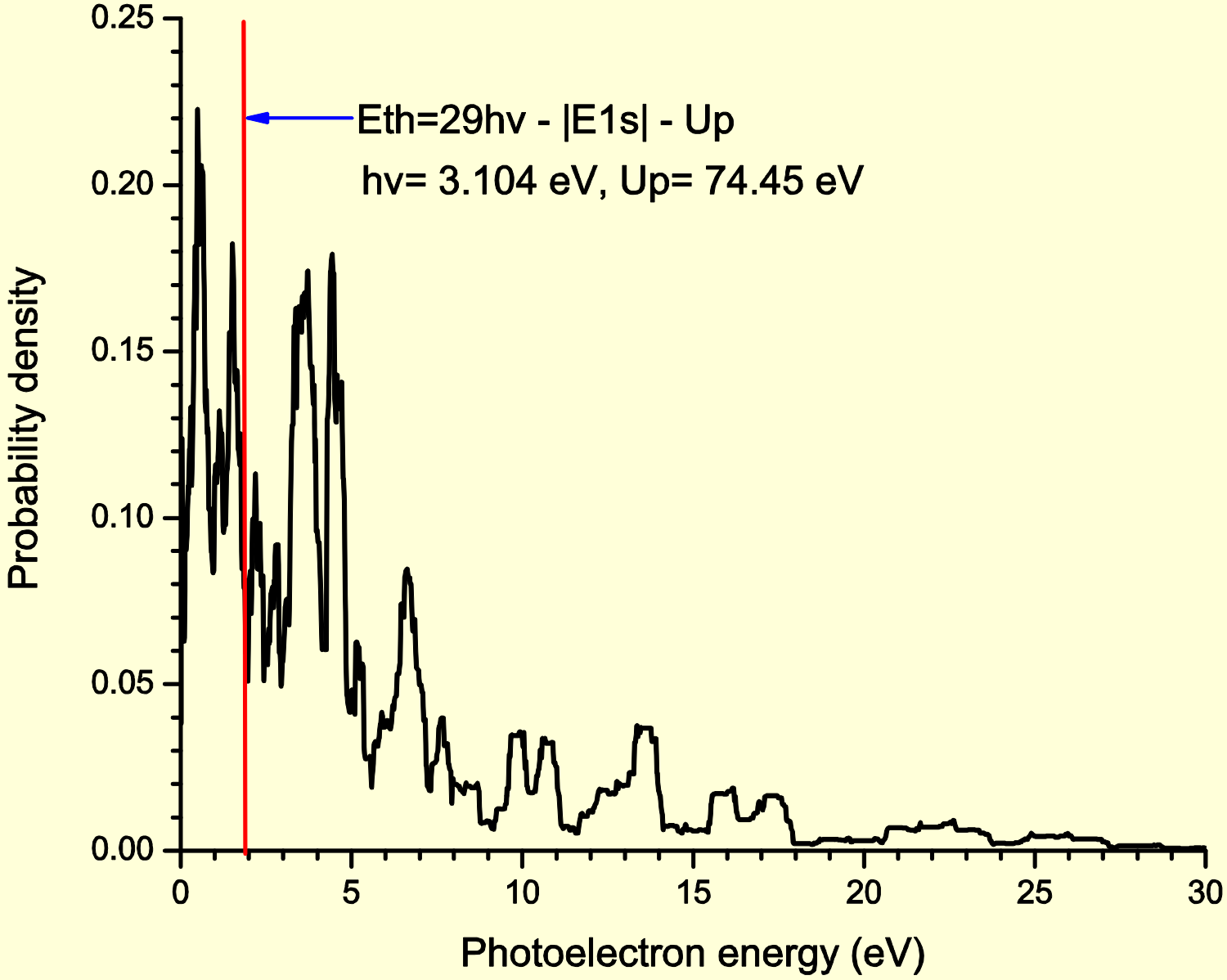
Eth=29hv - |E1s| - Up
hv= 3.104 eV, Up= 74.45 eV
Probability density
0.25
0.20
0.15
0.10
0.05
0.00
0
5
10
15
20
25
30
Photoelectron energy (eV)

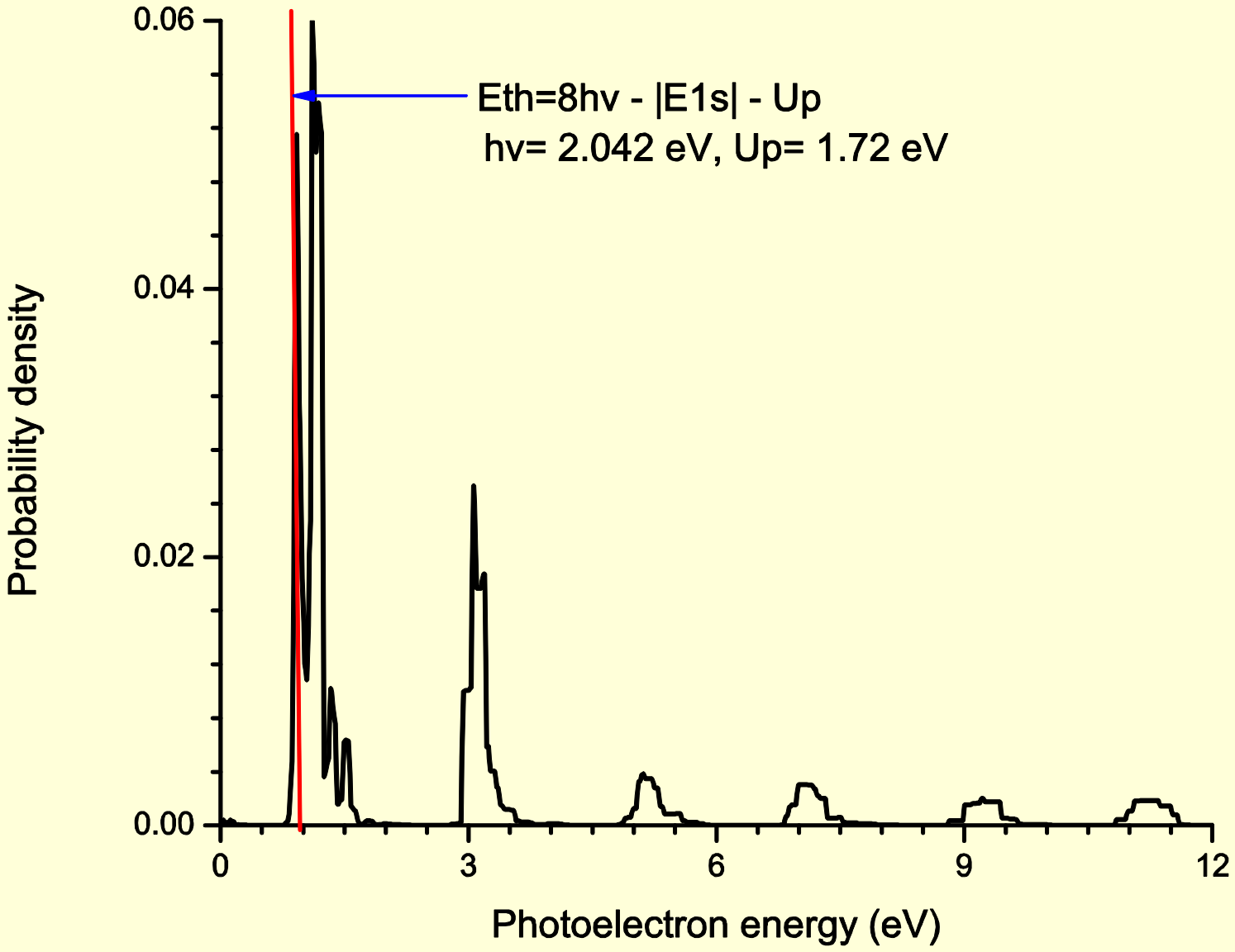
Eth=8hv - |E1s| - Up
hv= 2.042 eV, Up= 1.72 eV
Probability density
0.06
0.04
0.02
0.00
0
3
6
9
12
Photoelectron energy (eV)

Papers of our p-space work :

- Ue-Li Pena and T.F. Jiang, Phys Rev A46, 4297 (1992).
- T.F. Jiang, Phys Rev A48, 3995 (1993).
- Ue-Li Pen and T.F. Jiang. Phys Rev A53, 623 (1996).
- T.F. Jiang, Comp Phys Commun 178, 571 (2008).
- Zhen-Ting Huang et al, Comp Phys Commun 181,473 (2010).

SFA1 : Lewenstein model

- formulation

$$i\frac{\partial}{\partial t}|\Psi\rangle = \hat{H}(t)|\Psi\rangle \qquad H = H_0 + V_L$$

$$|\Psi(t)\rangle = -i\int_0^t dt' \left[e^{-i\int_{t'}^{t}\hat{H}(t'')\,dt''}\right]\hat{V}_{\mathrm{L}}(t')\left[e^{-i\int_0^{t'}\hat{H}_0(t'')\,dt''}\right]\times$$

$$\times\,|\Phi_{\mathrm{i}}\rangle + e^{-i\int_0^t \hat{H}_0(t'')\,dt''}|\Phi_{\mathrm{i}}\rangle$$

amplitude $a_{\mathbf{v}}(t)$ of populating the velocity $\mathbf{v}$ at the moment t is

$$a_{\mathbf{v}}(t) = -i\int_0^t dt' \langle \mathbf{v}|\left[e^{-i\int_{t'}^{t}\hat{H}(t'')\,dt''}\right]V_{\mathrm{L}}(t')\left[e^{-i\int_0^{t'}\hat{H}_0\,dt''}\right]|\Phi_{\mathrm{i}}\rangle$$

SFA1 : approximate the driven electron by neglecting the Coulomb potential

3-step model : tunneling, driven and recollision

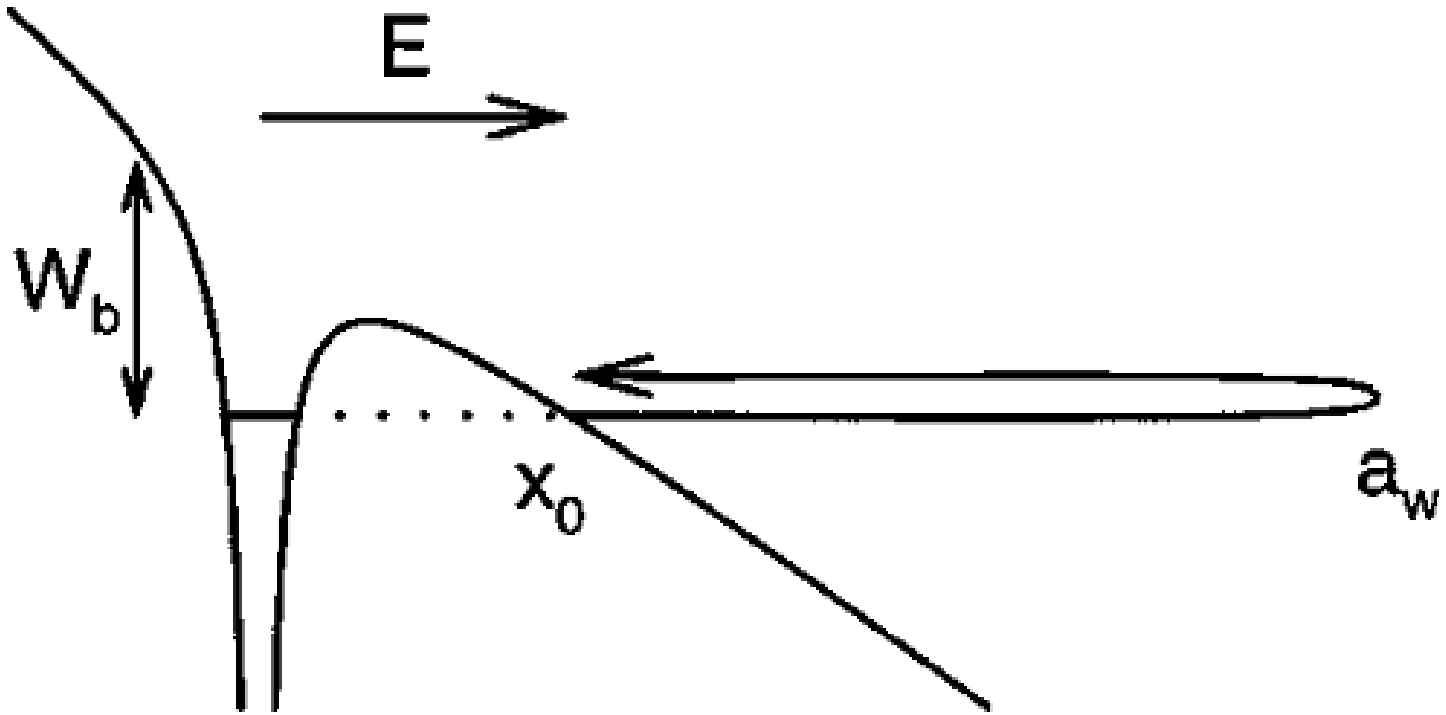

Recollision

Corkum (1993),
Kulander et al. (1993),
Lewenstein et al.(1994).

Classical theory I

- 3-step model

$$\ddot{z}(t) = -E_0 \cos \omega t,$$

$$z(t) = z(t_0) + \frac{E_0}{\omega^2}[\cos \omega t - \cos \omega t_0] + \left[\frac{E_0}{\omega}\sin \omega t_0 + \dot{z}(t_0)\right](t - t_0)$$

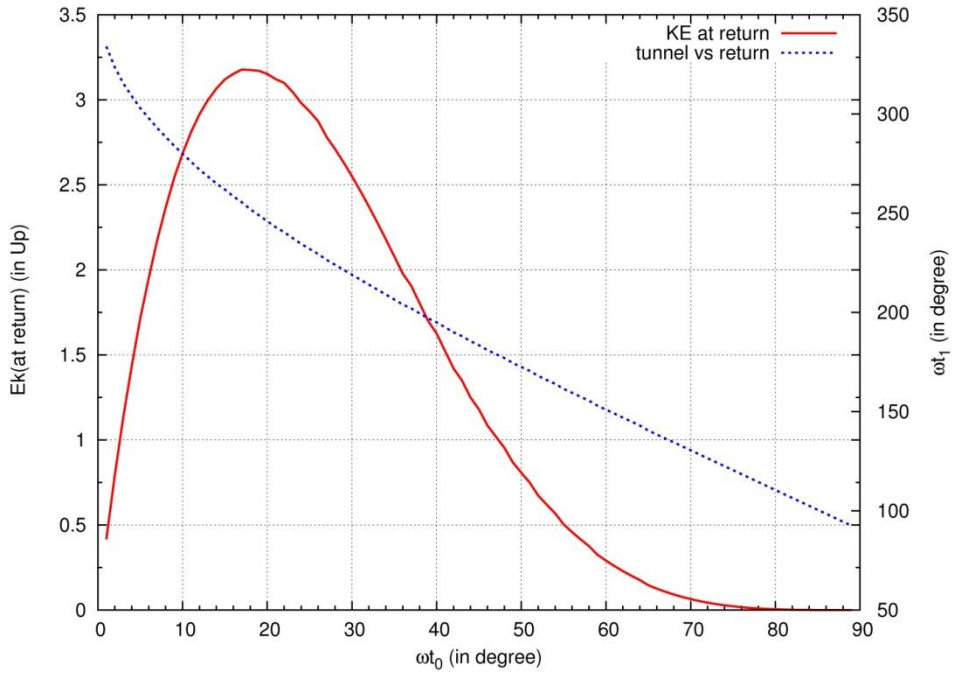

$$\cos \omega t_r - \cos \omega t_0 + \omega \sin \omega t_0 (t_r - t_0) = 0.$$

Maximum Ek(tr) ~ 3.17 Up

Cut-off order of HHG is ~ (3.17Up+Ip)/ω, an empirical fact.

SFA2 : rescattering model

$$f^{(2)} = -\int_{-\infty}^{\infty} dt \int_{-\infty}^{t} dt' \int d\mathbf{k} \langle \chi_{\mathbf{p}}(t) | V | \chi_{\mathbf{k}}(t) \rangle$$

$$\times \langle \chi_{\mathbf{k}}(t') | H_i(t') | \Psi_0(t') \rangle,$$

$H=T+V+H_i$, V is the atomic potential.
Initial electron kicked by laser and jump to continuous (approximated by Volkov) at t' , elastically rescattered by nucleus to $\boldsymbol{p}$ at t.

Volkov state approximation for continuous electron :

$$|\chi_{\mathbf{p}}(t)\rangle = |\mathbf{p} + \mathbf{A}(t)\rangle \exp[-iS_{\mathbf{p}}(t)]$$

$$S_{\mathbf{p}}(t) = \frac{1}{2}\int_{-\infty}^{t} dt' [\mathbf{p} + \mathbf{A}'(t)]^2$$

Classical theory II

- rescattering model

At return time, electron elastically rescattered by nucleus at angle ϑ_r to polarization axis.

$$\dot{z}(t) = -\frac{E_0}{\omega}[\sin\ \omega t - \sin\ \omega t_r + \cos\ \theta_r(\sin\ \omega t_r - \sin\ \omega t_0)]$$

$$\dot{y}(t) = -\frac{E_0}{\omega}\sin\ \theta_r(\sin\ \omega t_r - \sin\ \omega t_0).$$

$$E_k = 2U_p[\sin^2\ \omega t_0 + 2\ \sin\ \omega t_r(1 - \cos\ \theta_r)(\sin\ \omega t_r - \sin\ \omega t_0)]$$

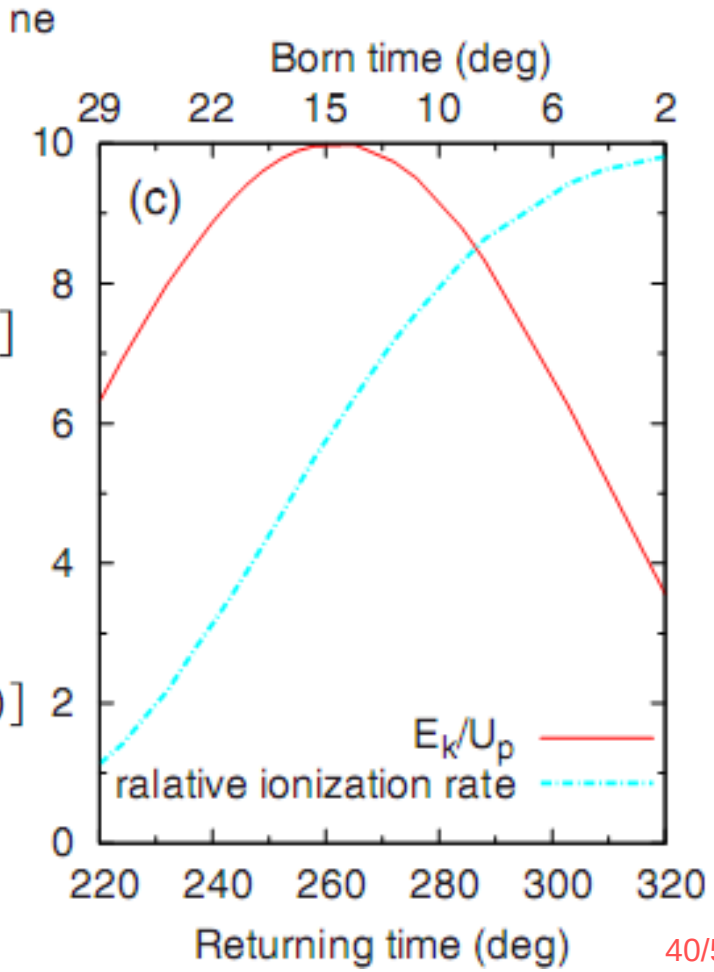

Maximum averaged rescattering Ek ~ 10.007 Up

CD Lin et al, 2009

Photoelectron spectra Ar TDSE vs SFA1

FIG. 2. (Color online) Photoelectron 2D momentum distributions for single ionization of argon by a 10-fs (FWHM) laser pulse with wavelength of 400 nm at the peak intensity of 3.2×10^{14} W/cm^2, calculated by the (a) full TDSE, (b) TDSE with r_c=5, (c) TDSE with r_c=2, and (d) SFA.

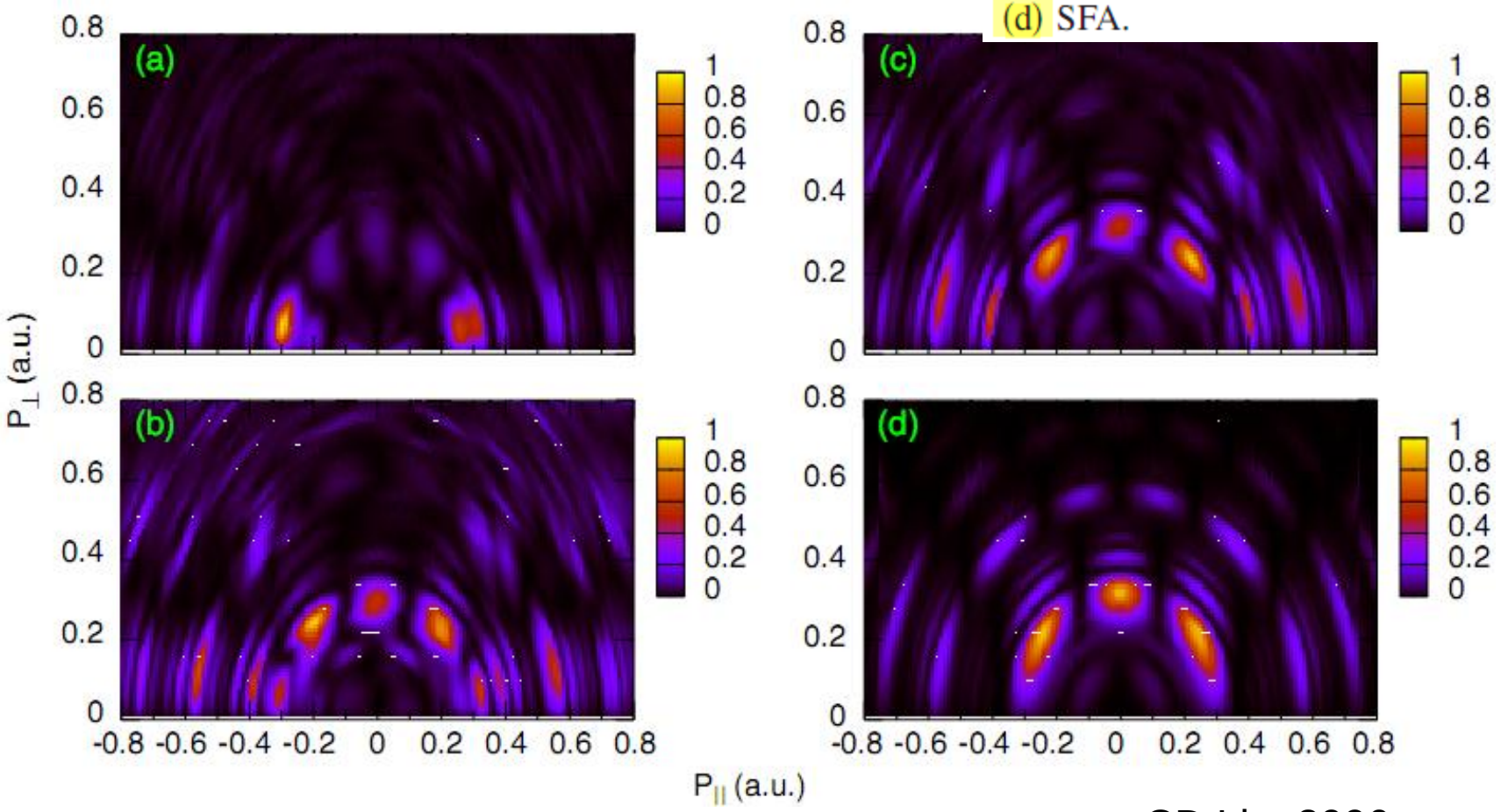

CD Lin, 2006

Results from SFA1 and SFA2 compared to TDSE

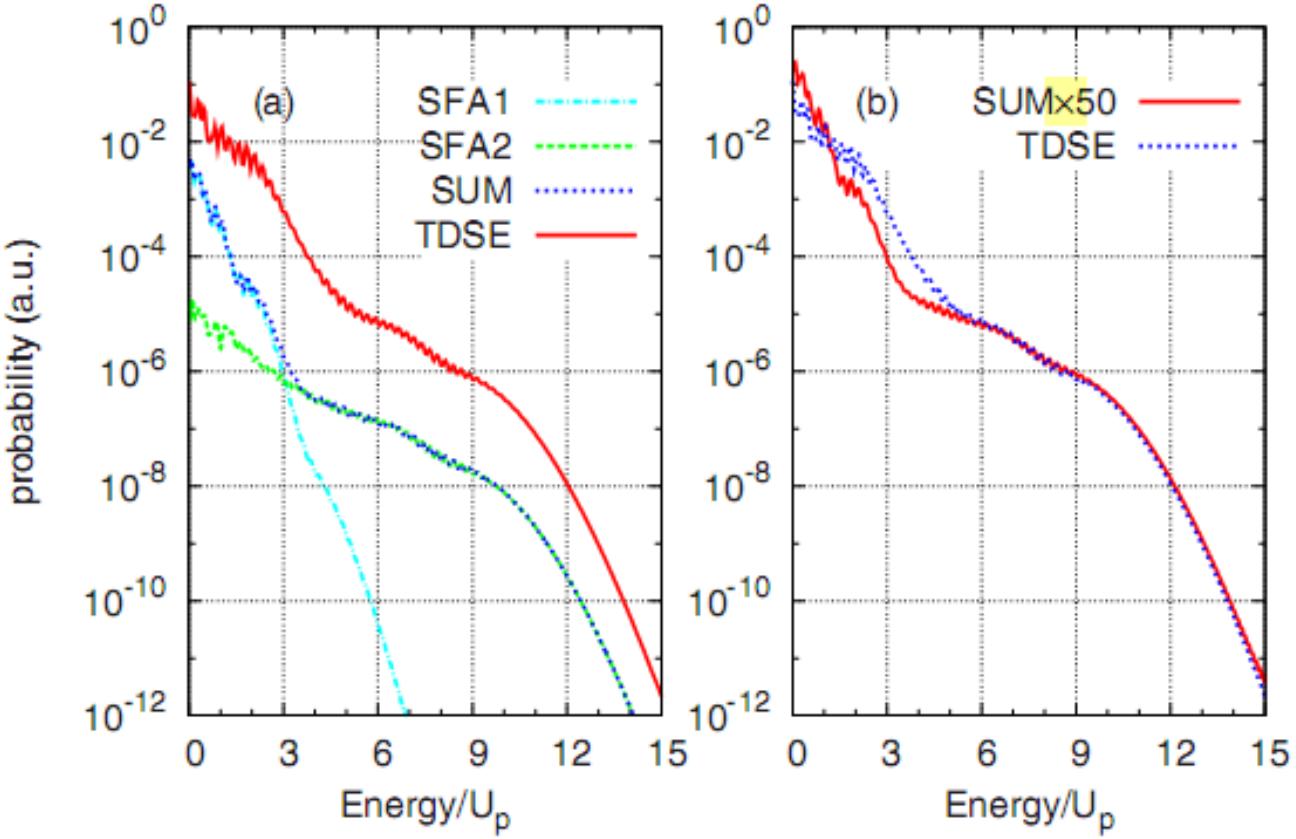

FIG. 1. (Color online) Electron energy spectra for atomic hydrogen by a five-cycle laser pulse with the wavelength of 800 nm at the peak intensity of 1.0×10^{14} W/cm^2. (a) From TDSE, first- (SFA1)

CD Lin et al, 2009

Higher energy spectra in rescattering picture :

classical : v(tf)= v(tr)+qA(tr)

"v(tr) is measured from the center of circle which is located at –A(tr)"

TDSE calculation

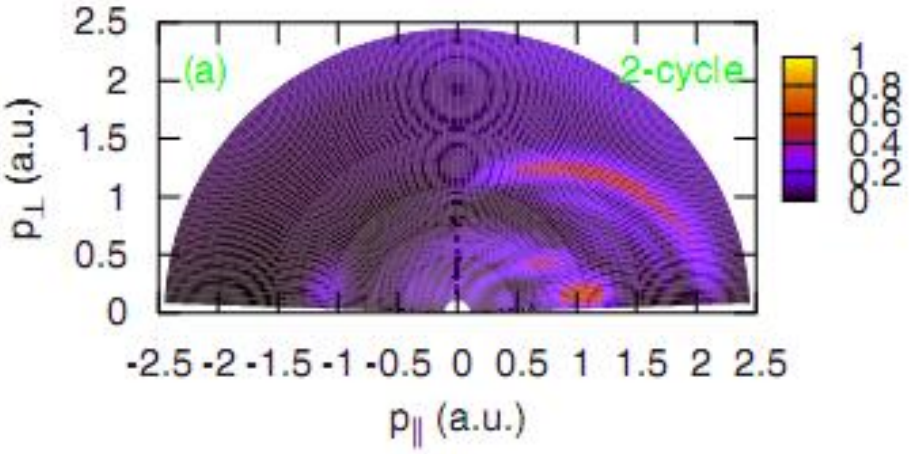

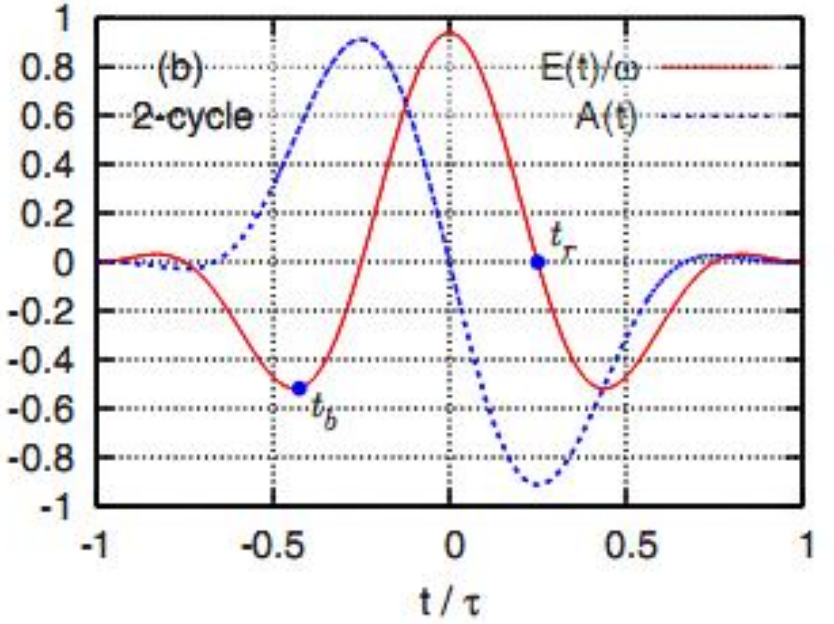

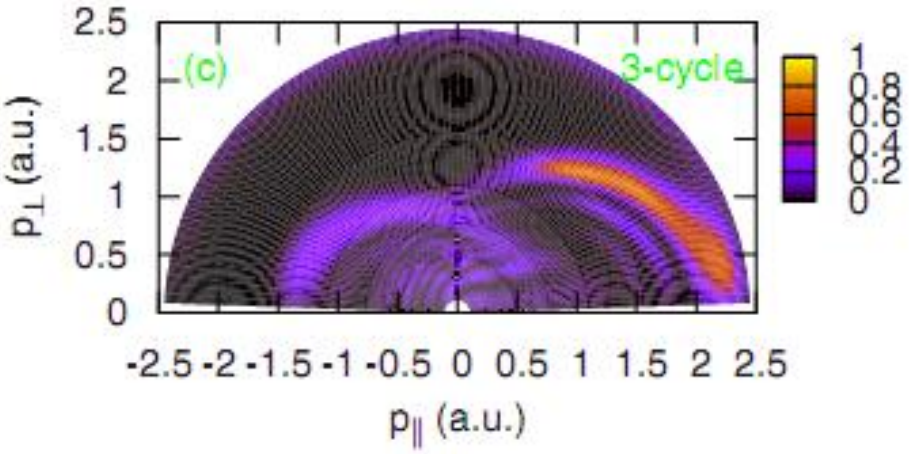

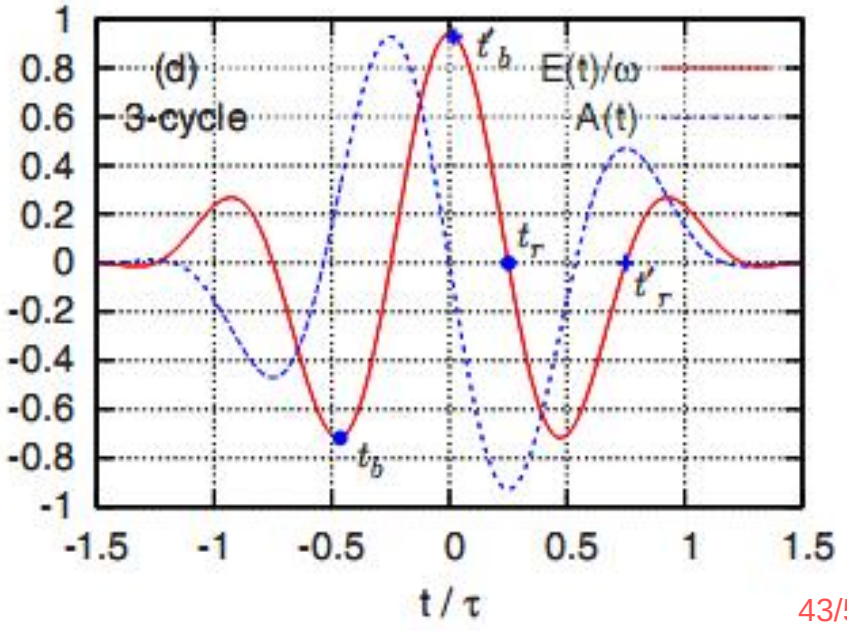

CD Lin et al, 2009

Molecular SFA

Under Born-Oppenheimer approx., diatomic SFA :

$$M_{\mathrm{fi}}^{q\mathrm{ML}}(t,t') = \sum_{J=\mathrm{A,B}} i\int_{t'}^{t} d\tau \int d^3\mathbf{r}d^3\mathbf{R}\,\phi^*_{\mathbf{e}\mathbf{p}_\mathrm{f}}(\mathbf{r},\tau)$$

$$\times\phi^*_{\mathrm{AB}\nu_\mathrm{f}}(\mathbf{R},\tau)(e_r\mathbf{r}+e_{R_J}\mathbf{R})\cdot\mathbf{E}(\tau)\Phi^q_{\mathrm{i}J}(\mathbf{r},\mathbf{R},\tau)$$

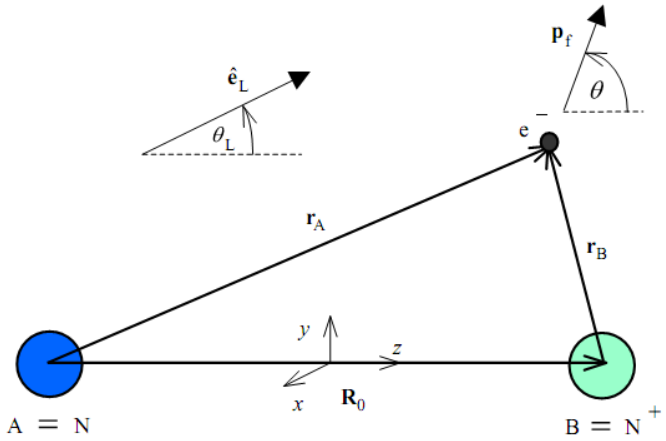

q means dressed or undressed**, r** is electron, **R** is nuclear coordinate. Molecule Kicked by laser at τ , molecule becomes excited and electron is in Volkov. From LCAO, laser can excite electron from atom A and B, there is interference from two paths. Molecular orbital symmetry is considered. Also SFA2 is developed. Both HHG and photoelectron can be calculated through SFA.

Faisal 2000
Milosevic 06,08,09
Chu 06
Madsen 06

Ionization alignment dependence, linear polarized, 800nm, 1 and 2×10^{14} w/cm^2

N_2, HOMO $3\sigma_g$, $2p_z(1)$-$2p_z(2)$

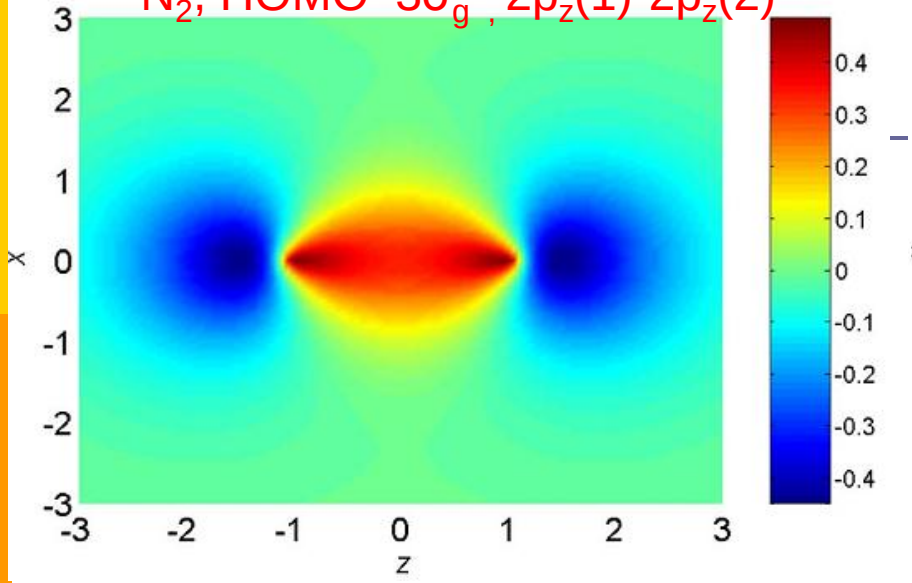

O_2 HOMO $1\pi_g$, $2p_x(1)$-$2p_x(2)$

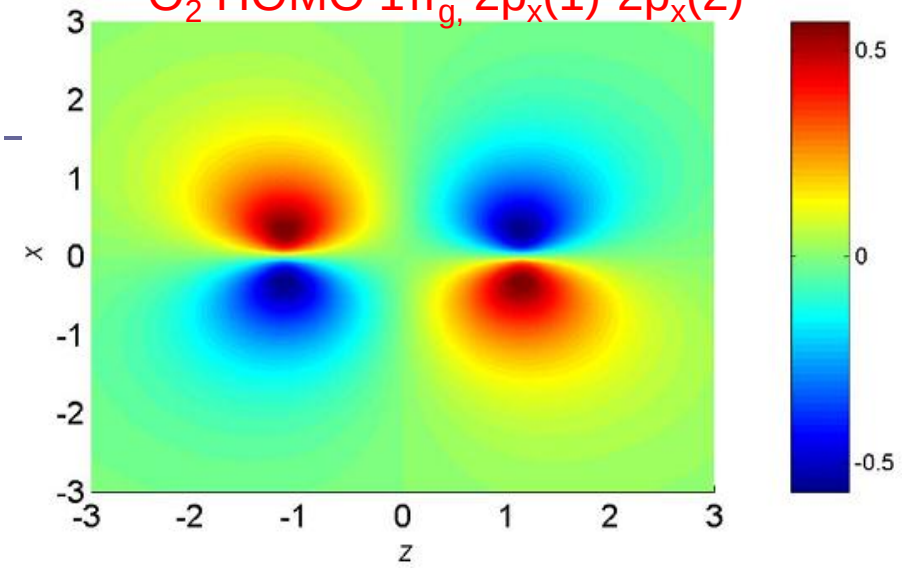

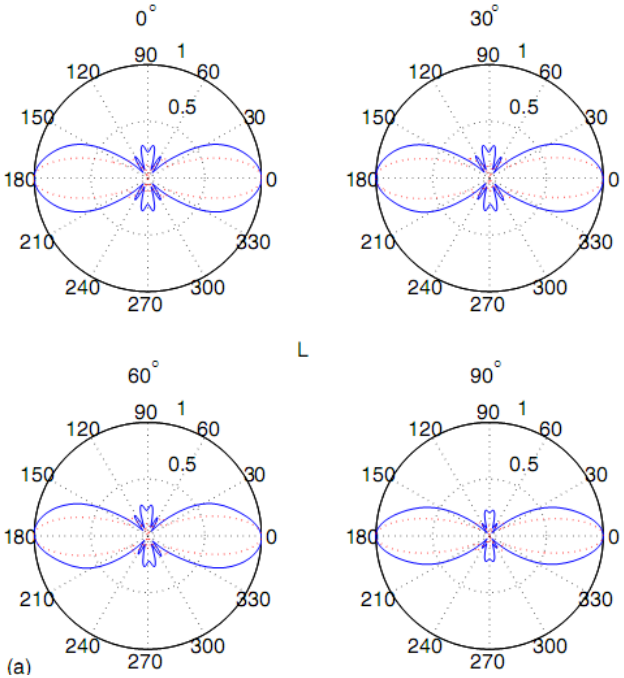

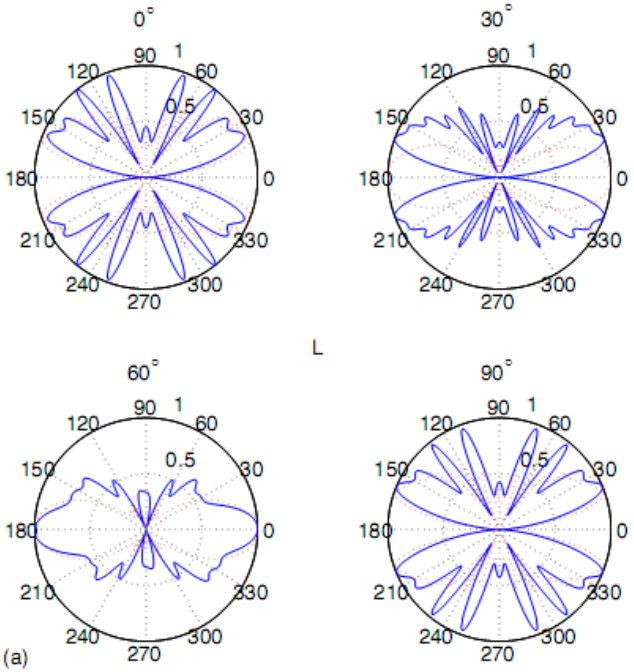

Personal comments on SFA

- SFA is simple and convenient tool, qualitative right for both atomic and molecular cases, and widely used.
- SFA1 lost Coulomb effect on photoelectron, spectrum is similar to TDSE with short-range potential at lower energy part but underestimated in ~two orders.
- SFA2 can describe higher energy electron, magnitude is underestimated, too.
- For molecular case, the validity is not clearly justified.
- An efficient and accurate enough method is demanding and important.

Pump-probe process on atom

Pump and probe pulse on top of each other.

See Tong 2010, Johnsson 2005,2007, Cocke 2010, Schafer 2004 etc.

The initial state free propagates to *t* and kicked by high frequency photon into continuous, and then propagates under IR laser field.

The study of laser assisted process goes back to Kroll, Watson (PRA8,804 (1973), Chu 77, Maquet etc. This problem is the old dressed atom picture but with new light pulse.

$$S = -i \int_{-\infty}^{+\infty} dt \left\langle \phi_{\mathbf{k}}(t) \left| \frac{1}{c} \mathbf{A}_X(t) \cdot \mathbf{p} \right| \phi_i(t) \right\rangle$$

S-matrix, perturbation theory

$\phi_i(t)$ is the dressed atomic state, calculated by perturbation theory

$\phi_k(t)$ is the dressed continuous state, a simple model is the Volkov, or more sophisticated state. See Cionga etc, PRA47,1830 (1993),Faisal 2005, Gayet etc, PRA66,023412(2002), Nakajuma etc , PRA75,043403 (2007), Yudin etc, JPB40,F93 (2010).

Simultaneously FEL + IR pump probe, theory and experiments on helium atom.

$$S = -\mathrm{i}\int_{-\infty}^{+\infty} \mathrm{d}t \langle \psi_{\mathbf{k}}(t)| \frac{1}{c}\mathbf{A}_X(t)\cdot\mathbf{p}|\psi_{1s^2}(t)\rangle \qquad \frac{1}{c}\mathbf{A}_X(t)\cdot\mathbf{p} = \frac{1}{c}A_{0X}\exp[-\mathrm{i}(\omega_X t+\phi_X)]\hat{\epsilon}_X\cdot\mathbf{p}.$$

long pulse as sinusoidal

$$\langle \mathbf{r}|\psi_{1s^2}(t)\rangle = \exp(-\mathrm{i}E_{1s^2}t)\psi_{1s^2}(\mathbf{r}) \qquad \langle \mathbf{r}|\psi_{\mathbf{k}}(t)\rangle = \exp\left(-\mathrm{i}\frac{1}{2}k^2 t\right)\psi_{\mathbf{k}}(\mathbf{r})$$

$$\langle \mathbf{r}|\chi_{\mathbf{k}}^{V}(t)\rangle = \exp\left[-\mathrm{i}\left(\boldsymbol{\alpha}(t)\cdot\mathbf{k}+\frac{1}{2}k^2 t\right)\right]\chi_{\mathbf{k}}(\mathbf{r}),$$

IR dressed

$$\boldsymbol{\alpha}(t) = \boldsymbol{\alpha}_0 \sin(\omega_L t+\phi_L); \quad \boldsymbol{\alpha}_0 = \frac{\mathbf{F}_{0L}}{\omega_L^2}$$

$$\chi_{\mathbf{k}}(\mathbf{r}) = \frac{1}{(2\pi)^{3/2}}\exp(\mathrm{i}\mathbf{k}\cdot\mathbf{r})$$

Jacobi-Anger formula :

$$\exp(\mathrm{i}z\sin\theta) = \sum_{n=-\infty}^{\infty} J_n(z)\exp(\mathrm{i}n\theta)$$

The Fourier–Bessel expansion of the exponential with sinusoidal argument yields:

$$\chi_{\mathbf{k}}^{V}(\mathbf{r},t) = \frac{1}{(2\pi)^{3/2}}\sum_{n=-\infty}^{+\infty} J_n(\boldsymbol{\alpha}_0\cdot\mathbf{k})\exp[-\mathrm{i}n(\omega_L t+\phi_L)]\exp\left[\mathrm{i}\left(\mathbf{k}\cdot\mathbf{r}-\frac{1}{2}k^2 t\right)\right], \qquad (9)$$

Then, replacing the S-matrix transition amplitude (2) and performing the time integration which leads to δ-function energy conservation terms, one gets

$$S = \sum_{n=-\infty}^{+\infty} S^{(n)} \delta\left(\frac{1}{2}k^2 - (E_{1s^2} + \omega_X + n\omega_L)\right), \tag{10}$$

$$S^{(n)} = -2\pi i J_{-n}(\boldsymbol{\alpha}_0 \cdot \mathbf{k}_n) \exp[-i(\phi_X + n\phi_L)]\langle \chi_{\mathbf{k}_n} | \epsilon_X \cdot \mathbf{p} | \psi_{1s^2} \rangle \tag{11}$$

with $k_n \approx [2(E_{1s^2} + \omega_X + n\omega_L)]^{1/2}$ is the shifted wave number of the ejected electron. cross-section corresponding to the exchange of n laser photons together with the absorption of the XUV photon, is

$$\left(\frac{d\sigma^{(n)}}{d\theta}\right)_{\tilde{E}_k} = J_n^2(\boldsymbol{\alpha}_0 \cdot \mathbf{k}_n)\left(\frac{d\sigma^{(0)}}{d\theta}\right)_{\tilde{E}_k}. \tag{12}$$

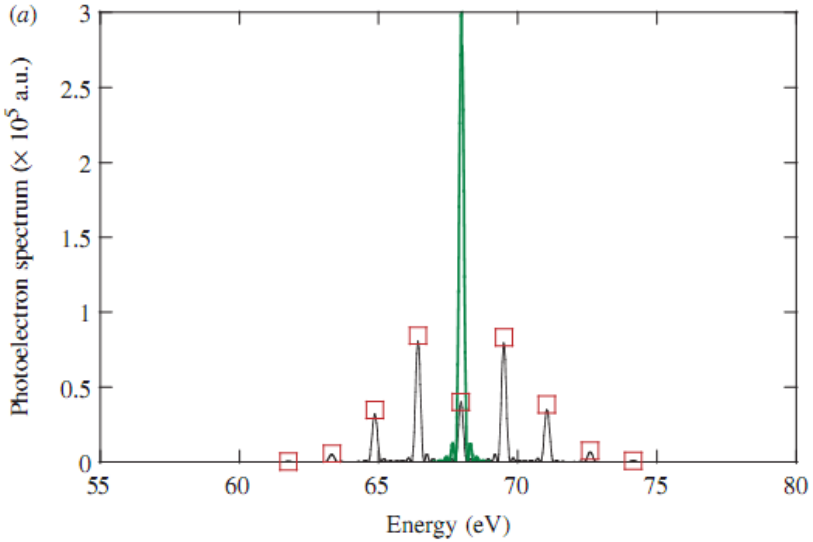

Field and target effects factorized !

Maquet, Taieb, J Mod Opt 54, 1847 (07)

photoionization of He. Angle-integrated spectra for $\omega_X = 92\,\text{eV}$ and $\omega_L = 1.55\,\text{eV}$ at different IR laser intensities, see text. Thin black line: TDSE calculation; red squares: soft-photon approximation. (*a*) $I_L = 5 \times 10^{11}\,\text{W cm}^{-2}$. The thick green line is the XUV single-photon

Conclusions

- Many activities of ultrashort, ultraintense laser pulses on various atoms, molecules, and pump probe experiments are undergoing.
- There are space for efficient and accurate theoretical methods besides SFA and TDSE.

Acknowledgements :

- Prof. Shih-I Chu (postdoctor 1988-9, visitor 1998-99 U of Kansas).
- Prof. Chii-Dong Lin and group members (visitor 2009,Kansas State Univ.).
- Prof. A.F. Starace (postdoctor 1985-6, U of Nebraska).
- Prof. N.N. Choi (Kumoh National Institute of Technology, Korea).
- Dr. Toru Morishita (Univ of Electrocommun. Tokyo).
- Dr. 李漢傑 (postdoctor)
- Mr. 鄭世達 (ph.d graduate)
- Mr. 吳明軒 (former ms graduates)

Thank you for attentions .